CONSTRUCTION MATERIALS CONSULTANTS, INC.

Laboratory Investigation Of A Precast Roof Assessment At The Biofilter Structure In Arauco Wood Manufacturing Plant In Moncure, North Carolina

Biofilter Roof Assessment At Arauco Wood Manufacturing Plant
Moncure, North Carolina

April 28, 2021
CMC 0321111

TABLE OF CONTENTS

EXECUTIVE SUMMARY

The present investigation centers around a 2-year-old biofilter at the Arauco Wood Manufacturing Plant in Moncure, North Carolina. The structure is 45′ × 165′ in plan area and includes 25′ tall cast-in-place reinforced concrete exterior walls and precast hollow core roof panels (HCPs) topped with a reinforced concrete slab (RCS). The function of the structure is to filter formaldehyde and exhaust from wood processing and manufacturing operations for pollution control. The hollow core roof panels (HCP) are the subject of this investigation. Eighty (80) HCPs form the roof structure in two (2) rows of forty (40). Each row spans about 21-feet between exterior walls and an interior wall. Panels are approximately 4-feet wide and 8-inches deep with six (6) evenly spaced 6-inch diameter cores and five (5) prestress tendons near the bottom of panel surfaces between cores. Hollow core panels are topped with a reinforced concrete slab (RCS) exposed at the roof surface without a waterproofing membrane. Exhaust processed by the Biofilter has a very low pH (acidic) and temperatures ranging from 150 to 200 degrees Fahrenheit during service. Formaldehyde levels within exhaust fumes are reportedly very high. Rapidly developing concrete deterioration was noticed soon after the beginning of service a few years ago. Protective coatings were applied, but these coatings also degraded rapidly. In 2019, XYPEX Megamix ii (cementitious overlay material with crystalline technology) was applied to interior wall surfaces following hydro-blasting. Megamix ii was not applied to HCP soffits. On-going deterioration of HCP soffits inside the tank have reportedly been observed since the beginning of service, including exposure of aggregate from degradation of cement paste.

As a result, three samples of hollow core panels (HCPs) marked as P-1, P-2 and P-3 were extracted from bottom side of HCPs through hollow core cells between tendons. All of these locations exhibited the same general degree of surface deterioration as described above. In addition, two composite cores, C-1 and C-2 were taken from roof concrete slab (RCS) through the hollow core panel (HCPs); C-1 was taken in a generally sound area whereas Core C-2 was taken on top of a crack exhibiting efflorescence. The RCS component was separated from the HCP at C-1 during coring, but at C-2 the RCS component is well-bonded to the HCP.

Based on the above background information provided, purposes of laboratory investigations are to determine: (a) the quality of concrete in the reinforced concrete slab (RCS) component in Core C-2 including evidence of any physical and/or chemical deterioration of concrete in RCS, and, of hollow core panel (HCP) component in Samples P-1 and P-3 from detailed petrographic examinations according to the procedures of ASTM C 856; (b) determine the extent of deterioration of concrete in the HCP component from the weathered brown undersides of the panels in Samples P-2 and P-3 from petrography and ion chromatography (latter according to the procedures of ASTM D 4327); and, (c) evaluate the hollow core panel components in Samples P-1 and P-3 for potential chemical attack, e.g., sulfate attack by ion chromatography and petrography.

Based on detailed petrographic examinations, the reinforced concrete roof top slab (RCS) component in Cores C-1 and C-2 are found to be compositionally similar and made using: (a) crushed basalt-andesite-trachyte series of volcanic rock coarse aggregate of nominal 1 in. (25 mm) sizes that are angular, dense, hard, well-graded, well-distributed and present in sound conditions; (b) crushed silica sand fine aggregate; (c) binary cementitious blend of major amount of Portland cement and subordinate amount of fly ash having a cementitious materials content estimated to be equivalent to 6 to $6^1/_2$ bags of Portland cement per cubic yard of which 10 to 15 percent is estimated to be fly ash, and water-cementitious materials ratios estimated to be 0.45 to 0.50 in the interior and slightly lower at the top $^1/_8$ in. of the densified finished surface region where finishing-induced densification has occurred to achieve the desired fine broom-finished surface of the roof top. The surface densification process was found to be an artifact of excessively air-entrained nature of RCS having an estimated 8 to 10 percent air.

Due to high air content the cast-in-place concrete in RCS was sticky, which has increased the difficulty to achieve a desirable fine broom-finish of the surface. Hence, there is evidence of prolonged finishing and finishing-induced densification of surface to create fine, short, elongated, discontinuous gaps or separations as incipient delamination within the top $^1/_8$ in. of the finished surface, which has the potential to develop large-scale delamination and separation of the densified finished surface from the interior main body. However, no such evidence of complete detachment of the air-free or low-air finished surface from the excessively air-entrained interior body is found in the RCS component in Cores C-1 or C-2. Therefore, excessive air in RCS has not only affected the overall compressive strength of concrete both from high air and the weakened aggregate-paste bond due to clustering of air at the aggregate-paste interfaces, but also affected the finishing operations to develop the potential for incipient delamination of the finished surface from the main body. Despite the reported lack of any surface delamination during field delamination survey, petrographic examinations of RCS in Cores C-1 and C-2 showed the potential for incipient delamination as short gaps or separations beneath the densified finished surface.

The hollow core panel (HCP) component in Cores C-1 and C-2 and in Samples P-1 and P-3 are compositionally similar and made using: (a) crushed granite coarse aggregate of nominal $^1/_2$ in. (12.5 mm) sizes that are angular, dense, hard, well-graded, well-distributed and present in sound conditions; (b) crushed silica sand fine aggregate; and (c) a hardened Portland cement paste having cement contents similar in all samples and estimated to be 7 to $7^1/_2$ bags per cubic yard, and water-cement ratios similar in all samples and estimated to be 0.40 to 0.45 in the interior bodies. Unlike RCS component, which is excessively air-entrained to have estimated 8 to 10 percent air, however, the HCP component in all samples show lack of air-entrainment having air contents estimated to be 2 to 3 percent.

The undersides of HCP in P-1, P-2, and P-3 showed weathered brown altered, carbonated and leached paste exposing the aggregate particles relative to paste due to interactions with exhaust materials, which has affected the 5 to 10 mm zone of the underside. Coarsely crystalline secondary calcite precipitates are found at the underside surfaces of HCP, which are precipitated on leached and carbonated and porous pastes extended to depths of 2 to 3 mm beyond which paste is denser, but still shows carbonation for a few millimeters before sound non-carbonated interior paste. Beyond the altered zone, the majority of the interior portions of HCP are present in dense, well-consolidated, and sound conditions without any physical or chemical deterioration.

Chemical alterations of HCPs are found to be confined to the 10 mm of underside beyond which the interior concretes showed no alterations of paste such as softening, increasing porosity from leaching or carbonation, which are all found only at the underside altered zones. Water-soluble chloride contents are consistent throughout the thickness of HCPs in Samples P-1 and P-3, but water-soluble sulfate contents showed a factor of 5 to 10 increase towards the mid-depth and altered zones compared to the sound concave interiors due to the reported exposures to hydrogen sulfide gas and related sulfate exposures during service. Despite such high sulfate at the altered zone, however, the interior concrete beyond the 5 to 10 mm altered zone is sound without any sulfate attack.

Major vertical crack extended through the entire thickness of RCS and HCP is seen in Core C-2 where the RCS component is well-bonded to HCP. By contrast, no cracking is found in RCS or HCP components in Core C-1 where the two components are completely de-bonded. Petrographic examinations of RCS or HCP found no evidence for any physical or chemical deterioration of concretes in these components to cause cracking. The vertical through-depth crack in Core C-2 is judged to be due to reasons not related to any deterioration in RCS and/or in HCP component. Perhaps, reasons such as the lack of control joints or expansion joints in the RCS have caused unaccommodative drying shrinkage cracking in RCS, which has extended not only through the RCS, but also through the HCP component, especially where the two components are well-bonded as in the case of Core C-2.

INTRODUCTION

Reported herein are the results of laboratory studies of concretes in the roof top cast-in-place reinforced concrete slab (RCS) and in the underlying hollow core panel (HCP) samples retrieved from a biofilter structure at Arauco Wood manufacturing plant located in Moncure, North Carolina.

BACKGROUND AND FIELD PHOTOGRAPHS

Structure and subject area: Biofilter structure at the Arauco wood manufacturing plant in Moncure, NC. The two-year-old structure is 45′ × 165′ in plan area and includes 25′ tall cast-in-place reinforced concrete exterior walls and precast hollow core roof panels (HCPs) topped with a reinforced concrete slab (RCS). The function of the structure is to filter formaldehyde and exhaust from wood processing and manufacturing operations for pollution control. The hollow core roof panels (HCP) are the subject of this investigation. Eighty (80) HCPs form the roof structure in two (2) rows of forty (40). Each row spans about 21-feet between exterior walls and an interior wall. Panels are approximately 4-feet wide and 8-inches deep with six (6) evenly spaced 6-inch diameter cores and five (5) prestress tendons near the bottom of panel surfaces between cores. Hollow core panels are topped with a reinforced concrete slab (RCS) exposed at the roof surface without a waterproofing membrane.

Environment inside tank: Exhaust processed by the Biofilter has a very low pH (acidic) and temperatures ranging from 150 to 200 degrees Fahrenheit during service. Formaldehyde levels within exhaust fumes are reportedly very high. Bacteria typically used to biologically degrade pollutants was not used when the structure was first commissioned for service. A system was installed to introduce bacteria into the treatment system, but it is unknown if bacteria levels are adequate. Lack of adequate bacteria has been communicated as a suspected contributor to the subject deterioration. Following were gasses detected by Arauco inside the tank using a Honeywell GasAlert Max XT II.

- Oxygen: 19.5 to 23.5%
- Flammability (LEL): < 10%
- Carbon Monoxide: < 35ppm
- Hydrogen Sulfide: < 10ppm

History: Rapidly developing concrete deterioration was noticed soon after the beginning of service a few years ago. Protective coatings were applied, but these coatings also degraded rapidly. In 2019, XYPEX Megamix ii (cementitious overlay material with crystalline technology) was applied to interior wall surfaces following hydro-blasting. Megamix ii was not applied to HCP soffits. On-going deterioration of HCP soffits inside the tank has reportedly been observed since the beginning of service, including exposure of aggregates from degradation of cement paste. A cursory visual review of a limited portion of the tank was reportedly conducted in October 2020 when deterioration of HCP soffits was confirmed. Further evaluation was recommended to confirm the depth, nature, and extent of distress including possible corrosion of pre-stress tendons near exposed soffits.

Following are some general findings from the field assessment:

a. Bottom sides of HCP panels exhibited surface deterioration throughout the tank. Exposed aggregate was observed sporadically throughout the tank where cementitious paste had eroded. In areas where paste was still present it was found to be soft and could be easily etched with a screwdriver. Paste appeared to be an orange color at HCP surfaces inside of the tank.
b. $^{7}/_{16}$″ diameter pre-stress tendons were generally measured 1-$^{1}/_{4}$″ from the bottom of HCPs. Excavations exposing tendons identified no signs of corrosion.
c. Liquid water drained from several HCP hollow core cells from excavations or drilled holes during the evaluation.
d. Half-cell potential testing was performed at seven (7) locations along tendons. Testing did not identify spikes in negative potential typically indicative of corrosion activity.
e. No concrete delaminations, spalls or cracks were identified.
f. The roof slab topping the HCP panels was found to be 3-$^{1}/_{4}$″ thick and reinforced with #4 bars at 16″ o.c. both ways. The slab exhibited frequent cracking parallel with HCP joints, map-type cracking near the middle of the roof and random diagonal cracking throughout the roof area. Efflorescence and light orange staining were identified around some cracks.

The roof slab was sounded via chain dragging. No near-surface delaminations were detected. Scaling was not observed on the fine broom-finished surface of roof top slab. Visible cracks were observed on the roof top slab, which are typically either coincident with HCP joint locations or random cracks that were typically long and meandering. Much of these cracks are reportedly of the type expected from lack of proper jointing. Since the slab is only 2-3 years old, near-surface delamination, if present, are incipient which may manifest to larges scales with time.

Sample Locations: Samples P-1, P-2, and P-3 were extracted from bottom side of HCPs through hollow core cells between tendons. All of these locations exhibited the same general degree of surface deterioration as described above. Cores C-1 and C-2 were taken from roof slab. Cores penetrate through the roof slab and through the top-side of the HCPs at hollow core cells. Core C-1 was taken in a generally sound area; Core C-2 was taken on top of a crack exhibiting efflorescence. The topping slab separated from the top surface of the HCP at C-1 during coring, but at C-2 the topping slab remained bonded forming a composite sample.

PURPOSE

Based on the above background information provided, purposes of laboratory investigations are to determine:

a. The quality of concrete in the reinforced concrete slab (RCS) component in Core C-2 including evidence of any physical and/or chemical deterioration of concrete in RCS, and, of hollow core panel (HCP) component in Samples P-1 and P-3 from detailed petrographic examinations according to the procedures of ASTM C 856;

b. Determine the extent of deterioration of concrete in the HCP component from the weathered brown undersides of the panels in Samples P-2 and P-3 from petrography and ion chromatography (latter according to the procedures of ASTM D 4327); and,

c. Evaluate the hollow core panel components in Samples P-1 and P-3 for potential chemical attack, e.g., sulfate attack from ion chromatography and petrography.

Biofilter Structure at the Arauco Wood Manufacturing Plant in Moncure, NC

The two-year old structure is 45′ by 165′ in plan area and includes 25′ tall cast-in-place reinforced concrete exterior walls and precast hollow core roof panels (HCPs) topped with a reinforced concrete slab. The function of the structure is to filter formaldehyde and exhaust from wood processing and manufacturing operations for pollution control. The HCPs are the subject of this evaluation.

Figure 1: The biofilter at Arauco Wood Manufacturing Plant containing a 25 ft. tall cast-in-place reinforced concrete exterior walls and precast hollow core roof panels (HCPs) topped with a reinforced concrete slab (RCS).

Biofilter Structure at the Arauco Wood Manufacturing Plant in Moncure, NC

Environment inside tank: Exhaust processed by the Biofilter has a very low pH and temperatures ranging from 150 to 200 degrees Fahrenheit during service. Formaldehyde levels within exhaust fumes are reportedly very high. Bacteria typically used to biologically degrade pollutants was not used when the structure was first commissioned for service; a system was installed to introduce bacteria into the treatment system, but it is unknown if bacteria levels are adequate. Lack of adequate bacteria has been communicated as a suspected contributor to the subject deterioration. Following were gasses detected by Arauco inside the tank using a Honeywell GasAlert Max XT II. Oxygen: 19.5 to 23.5% Flammability (LEL): < 10% Carbon Monoxide: < 35ppm Hyrdrogen Sulfide: < 10ppm

History: Rapidly developing concrete deterioration was noticed soon after the beginning of service a few years ago. Protective coatings were applied, but these coatings also degraded rapidly. In 2019, XYPEX Megamix ii (cementitious overlay material with crystalline technology) was applied to interior wall surfaces following hydro-blasting. Megamix ii was not applied to HCP soffits. On-going deterioration of HCP soffits inside the tank has reportedly been observed since the beginning of service, including exposure of aggregate from degradation of cement paste. SKA performed a cursory visual review of a limited portion of the tank in October 2020 during which deterioration of HCP soffits was confirmed. SKA recommended further evaluation to confirm the depth, nature and extent of distress including possible corrosion of pre-stress tendons near exposed soffits.

Figure 2: Field photos of the condition of inside of tank showing concrete deterioration of interior wall surfaces, despite reported application of protective coatings.

Biofilter structure at the Arauco Wood Manufacturing Plant in Moncure, NC

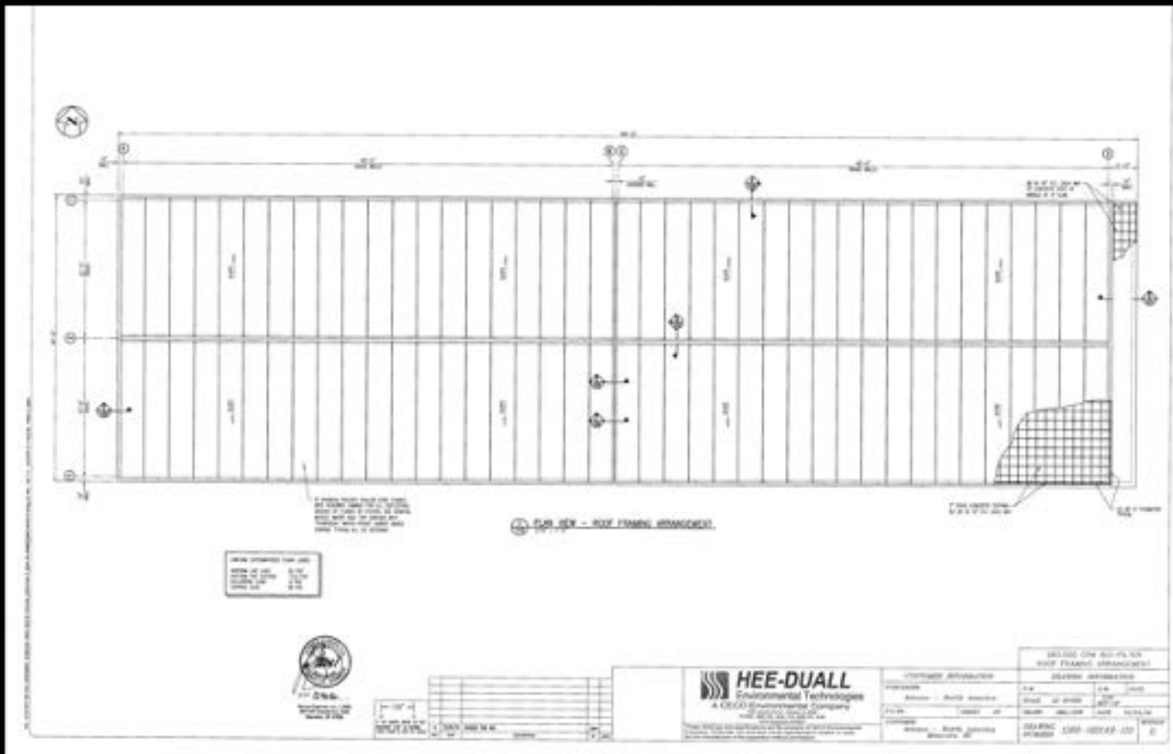

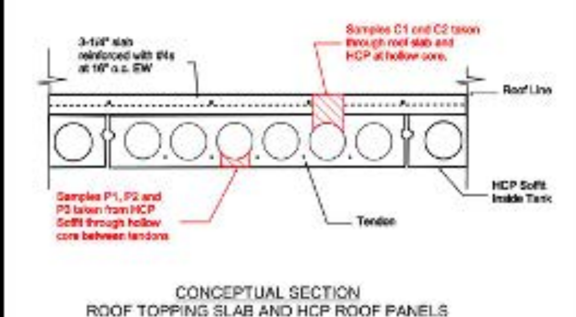

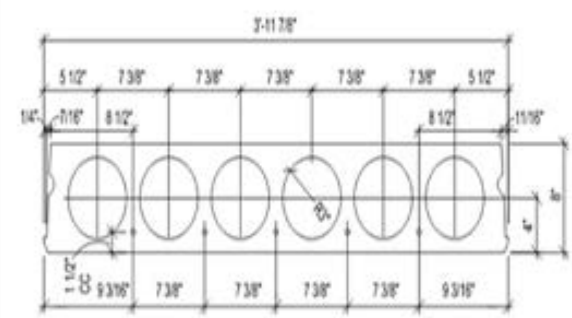

Eighty (80) HCPs form the roof structure in two (2) rows of forty (40). Each row spans about 21-feet between exterior walls and an interior wall. Panels are approximately 4-feet wide and 8-inches deep with six (6) evenly spaced 6-inch diameter cores and five (5) prestress tendons near the bottom of panels surfaces between cores. Hollow core panels are topped with a reinforced concrete slab exposed at the roof surface without a waterproofing membrane.

Figure 3: Relevant drawings of structure consisting of eighty HCPs forming the roof structure in two rows of forty panels. HCPs are topped with a reinforced concrete slab exposed at the roof surface without a waterproofing membrane.

METHODOLOGIES

PETROGRAPHIC EXAMINATIONS

The cores were examined using the methods and procedures of ASTM C 856 "Standard Practice for Petrographic Examination of Hardened Concrete." Details of concrete petrography, and sample preparation techniques for petrographic examinations of concrete are provided in Jana (2006).

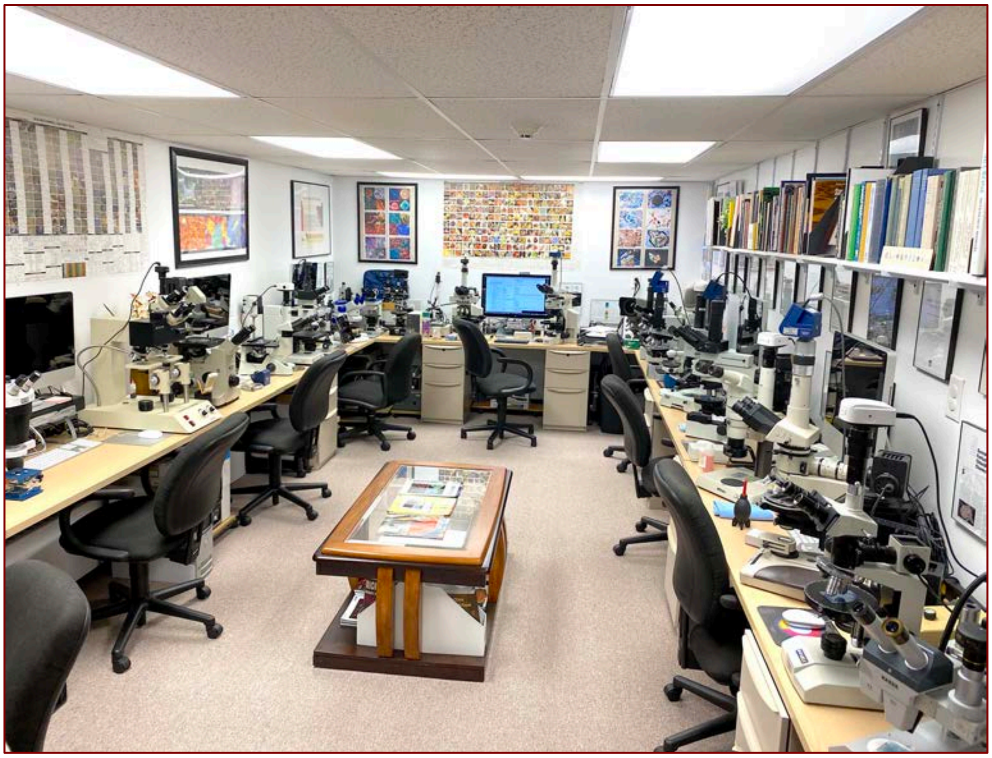

Figure 4: Some of the optical microscopes in the optical microscopy laboratory that were used for this investigation, e.g., from low-power stereo microscope, to high-power transmitted-light stereo-zoom microscope with plane and crossed-polarized light, to epi-fluorescent microscope for observations of florescent dye-mixed epoxy impregnated thin sections and petrographic microscopes for further observations of thin sections of concretes.

Briefly, the steps followed during petrographic examination of samples include:

i. Visual examinations of the concretes, as received, including adequate documentation of dimensions, measurements, condition, physical properties, integrity, etc.;
ii. Low-power stereo microscopical examinations of as-received, saw-cut and freshly fractured sections, and lapped cross sections of samples for evaluation of texture, air-void systems, and compositions;
iii. Examinations of oil immersion mounts in a petrographic microscope for mineralogical compositions of specific areas of interests;
iv. Examinations of fluorescent dye-mixed (to highlight open spaces, cracks, etc.) low-viscosity epoxy-impregnated large area (50 mm × 75 mm) thin sections of concretes in a petrographic microscope for detailed compositional and microstructural analyses;
v. Photographing the samples, as received and at various stages of preparation with a digital camera and a flatbed scanner; and,
vi. Photomicrographs of lapped sections and thin sections of concretes taken with stereomicroscope and petrographic microscope, respectively to provide detailed compositional and mineralogical information of concretes.

ANALYSES OF WATER-SOLUBLE ANION CONTENTS

Water-Soluble anion (e.g., chloride, sulfate) contents of hollow core panel (HCP) components in Samples P-1 and P-3 were determined by ion chromatography according to the procedures of ASTM D 4327. Analyses were done on the pulverized portions of saw-cut sections of HCPs taken from the altered undersides, the mid-depth locations, and concave ends.

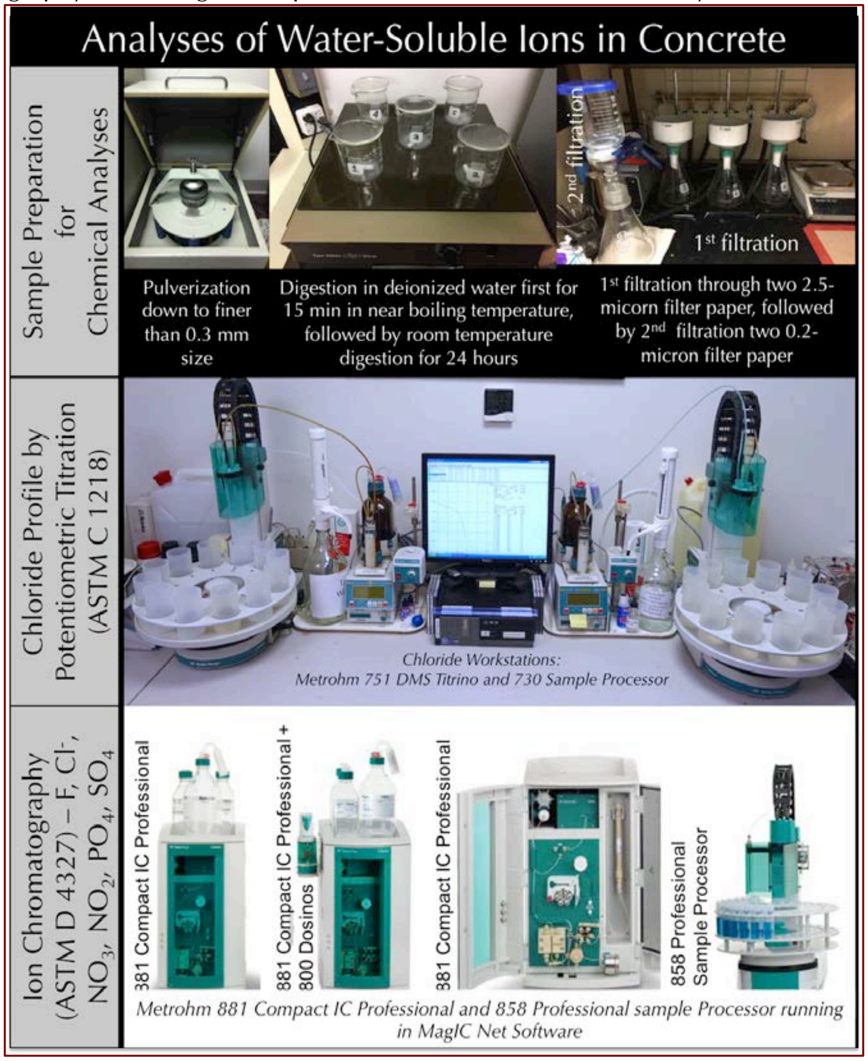

Figure 5: Sample preparation and analyses of water-soluble ions of by ion chromatography.

The sample preparation steps were similar to that of water-soluble chloride contents in concrete according to the methods of ASTM C 1218: "Standard Test Method for Water-Soluble Chloride in Mortar and Concrete."

Steps followed in water-soluble anion contents by ion chromatography are as follows:

- Sample Selection and Sectioning – A representative portion of each core from the desired depth was sectioned and pulverized to fine powder passing US No. 50 sieve.
- Water Digestion – About 10±0.01 gm. of powder sample was measured and dispersed with 100-mL deionized water in a 250-mL beaker, stirring and breaking up any lumps with a glass rod.
- Further Digestion in Boiling Water – Covered the beaker from previous step with a watch glass, and heated rapidly to boiling, but not more than 10 minutes. Removed from hot plate.
- Filtration – Filtered the sample solution, under suction, through two 2.5 micron filter papers fitted to a Buchner funnel in a 500-mL filtration flask. Transferred the filtrate from the flask to the original beaker, which was already rinsed twice with water, along with the flask. Cooled the filtrate to room temperature. The final volume was 200-mL.
- Filtrates of water-digested samples were used for determination of various anions by ion chromatography (IC) by following the methods of ASTM D 4327 for anion chromatography, *a la* ASTM D 4327 for water-soluble fluoride, chloride, nitrate, nitrite, bromide, phosphate, and sulfate ions by using Metrohm 881 Compact IC Professional with attached 858 Professional Sample Processor with a sodium carbonate-bicarbonate eluent.
- In IC, ppm-chloride is converted to weight percent by weight% Cl = [(ppm-Cl from IC × Filtrate Volume 200 ml × Dilution Factor) / (Sample weight, 10 grams × 10,000)].

SAMPLES

Two composite cores, C-1 and C-2, each containing a roof top reinforcing concrete slab (RCS) component and an underlying hollow core panel (HCP) component, and, three separate saw-cut sections of hollow core panels (HCP) in samples P-1, P-2, and P-3 were received, which are described below.

Sample ID	Dimensions	Thickness	Top Exposed Surface	Bottom Surface	Cracking	Reinforcing Steel	Core Condition
Core C-1 (Figure 6)	Core Diameter - 4 in. (100 mm)	Roof top concrete slab (RCS) $3\frac{3}{8}$ in. (83 mm), and Hollow Core Panel (HCP) $1\frac{1}{4}$ in. to $2\frac{1}{2}$ in. (35 to 60 mm)	Fine broom-finished surface of RCS surface, no visible distress or cracking	Curved concave surface of HCP	None	None	RCS is de-bonded from HCP; Both are Intact, Dry, Ring
Core C-2 (Figure 7)	Core Diameter - 4 in. (100 mm)	Roof top concrete slab (RCS) $3\frac{3}{8}$ in. (83 mm), and Hollow Core Panel (HCP) $1\frac{1}{8}$ in. to $2\frac{1}{2}$ in. (30 to 60 mm)	Fine broom-finished surface of RCS surface, with vertical through-depth crack	Curved concave surface of HCP	Major vertical through-depth crack extended through the entire thickness of RCS and HCP	No. 4 reinforcing steel at 1 in. depth in RCS component	RCS is well-bonded to HCP; Both are Intact, Dry, Ring
Sample P-1 (Figure 8)	$5\frac{3}{4}$ in. × $3\frac{1}{2}$ in. × 2 in. (150 mm × 90 mm × 50 mm)	Only HCP component which is 2 in. thick	Sound concave white surface of HCP	Weathered brown altered underside of HCP, aggregates are exposed relative to paste	None	None	Intact, Dry, Ring
Sample P-2 (Figure 9)	$6\frac{5}{8}$ in. × $4\frac{1}{2}$ in. × $2\frac{1}{2}$ in. (168 mm × 120 mm × 60 mm)	Only HCP component which is 2 in. thick	Sound concave white surface of HCP	Weathered brown altered underside of HCP aggregates are exposed relative to paste	None	None	Intact, Dry, Ring
Sample P-3 (Figure 10)	6 in. × $3\frac{1}{2}$ in. × $1\frac{1}{2}$ in. (150 mm × 90 mm × 40 mm)	Only HCP component which is $1\frac{1}{2}$ in. thick	Sound concave white surface of HCP	Weathered brown altered underside of HCP aggregates are exposed relative to paste	None	None	Intact, Dry, Ring

Table 1: Detailed preliminary descriptions and dimensions of samples, as received.

Figure 6: Core C-1 as received showing top exposed sound, fine broom-finished surface of reinforced concrete slab (RCS) at the top left with some edge scaling of concrete, concave underside of hollow core panel (HCP) at the bottom half of core in top right photo, and de-bonded interface of two components, the RCS at the top and HCP at the bottom, with typical concave surface of interior of HCP. Core was reportedly taken from a sound area.

Figure 7: Core C-2 as received showing top exposed cracked, fine broom-finished surface of reinforced concrete slab (RCS) at the top left with a long continuous surface crack and discoloration of surface along the crack, concave underside of hollow core panel (HCP) at the bottom half of core in top right photo, and bonded interface of two components, the RCS at the top and HCP at the bottom with typical concave surface of interior of HCP where the surface crack has vertically transected through both components throughout the depth of the core. Core was reportedly taken from the top of a surface crack exhibiting efflorescence.

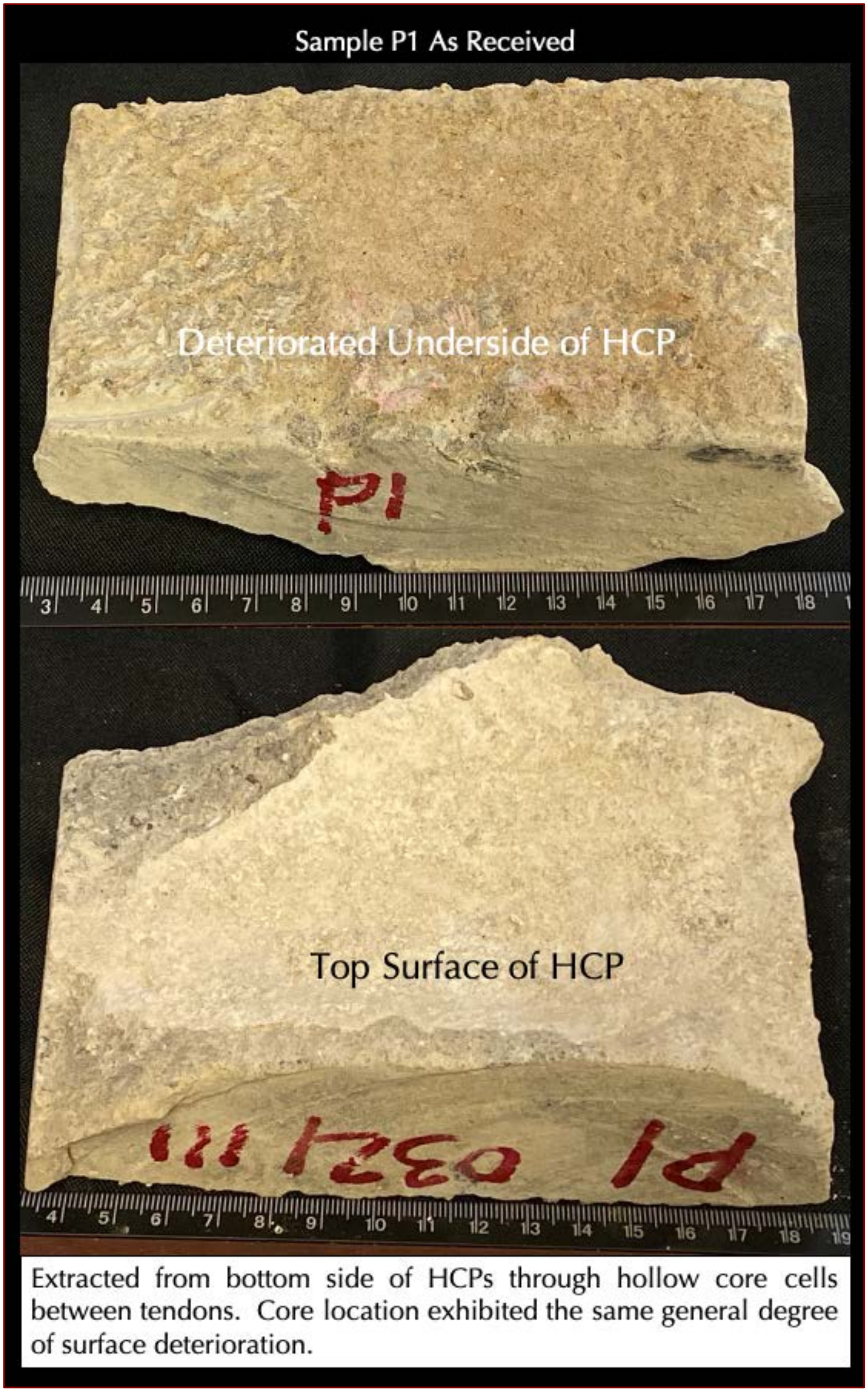

Figure 8: Portion of hollow core panel (HCP) received in Sample P-1 showing the overall brown, weathered, rough deteriorated underside of the HCP in the top photo and concave top surface of HCP in the bottom photo.

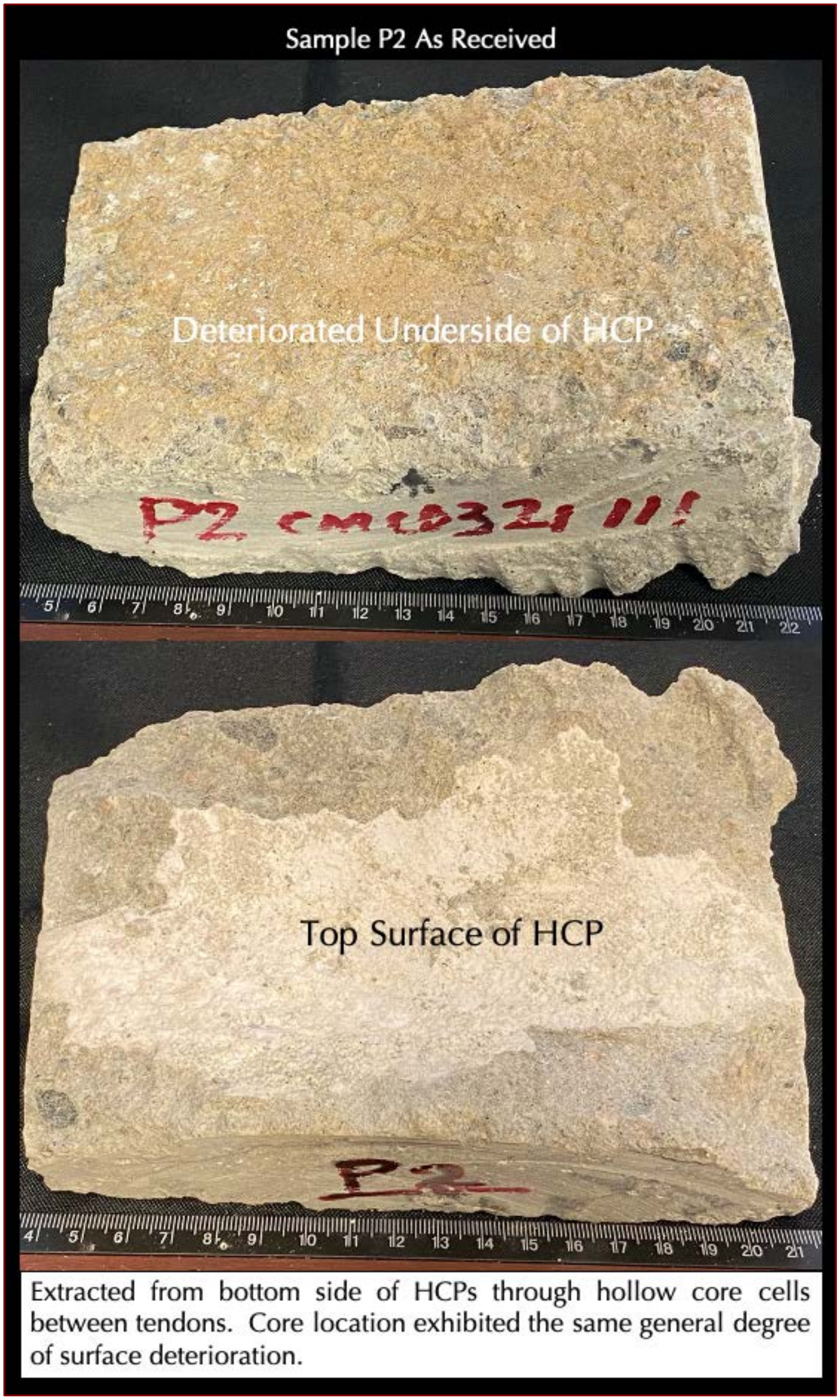

Figure 9: Portion of hollow core panel (HCP) received in Sample P-2 showing the overall brown, weathered, rough deteriorated underside of the HCP in the top photo and concave top surface of HCP in the bottom photo. All three samples of HCP in P-1, P-2, and P-3 show brown discoloration and rough altered weathered underside with exposures of aggregate particles against alerted paste, which is a common microstructural feature that forms due to higher dissolution of interstitial paste compared to aggregates, typically found in concretes exposed to acidic solutions as in sewer environments.

Figure 10: Portion of hollow core panel (HCP) received in Sample P-3 showing the overall brown, weathered, rough deteriorated underside of the HCP in the top photo and concave top surface of HCP in the bottom photo. All three samples of HCP in P-1, P-2, and P-3 show brown discoloration and rough altered weathered underside with exposures of aggregate particles against alerted paste, which is a common microstructural feature forms due to higher dissolution of interstitial paste compared to aggregates, typically found in concretes exposed to acidic solutions as in sewer environments.

PETROGRAPHIC EXAMINATIONS

LAPPED CROSS SECTIONS

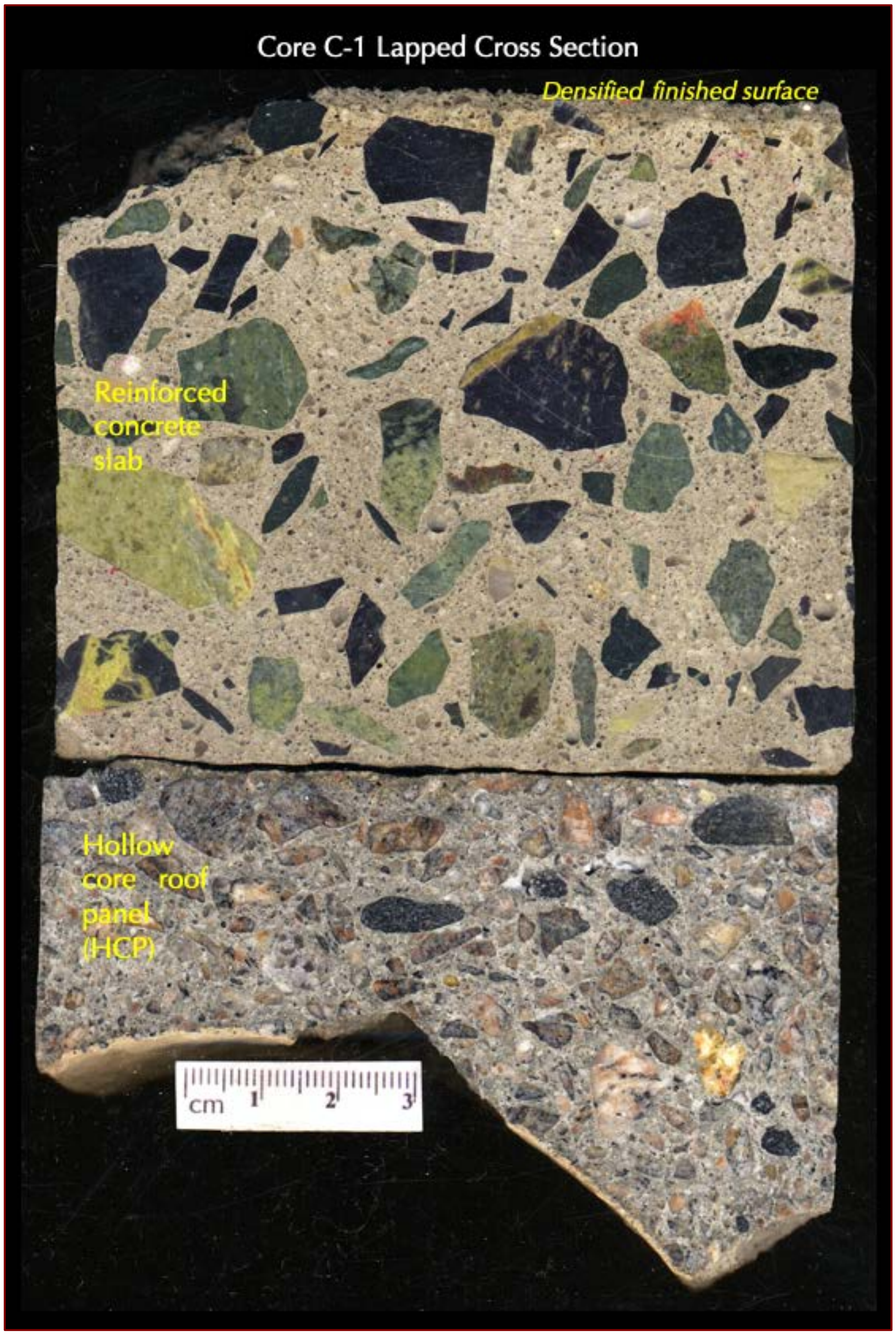

Figure 11: Lapped cross section of Core C-1 showing: (a) the reinforced concrete slab (RCS) at the top, completely de-bonded from the hollow core roof panel (HCP) at the bottom; (b) crushed volcanic stone coarse aggregate of 1 in. (25 mm) nominal size in RCS as opposed to crushed granite coarse aggregate of 1/2 in. (12.5 mm) nominal size in HCP; (c) medium beige color tone of paste in RCS as opposed to darker gray paste in HCP; (d) densified finished surface of RCS at the top 1/8 in.; (e) relatively better grading of crushed granite coarse aggregate in HCP as opposed to crushed volcanic rock coarse aggregate in RCS; (f) overall dense and well-consolidated natures of RCS and HCP concretes; and (g) relatively clear separation of RCS from HCP with no trace of one adhered to the other.

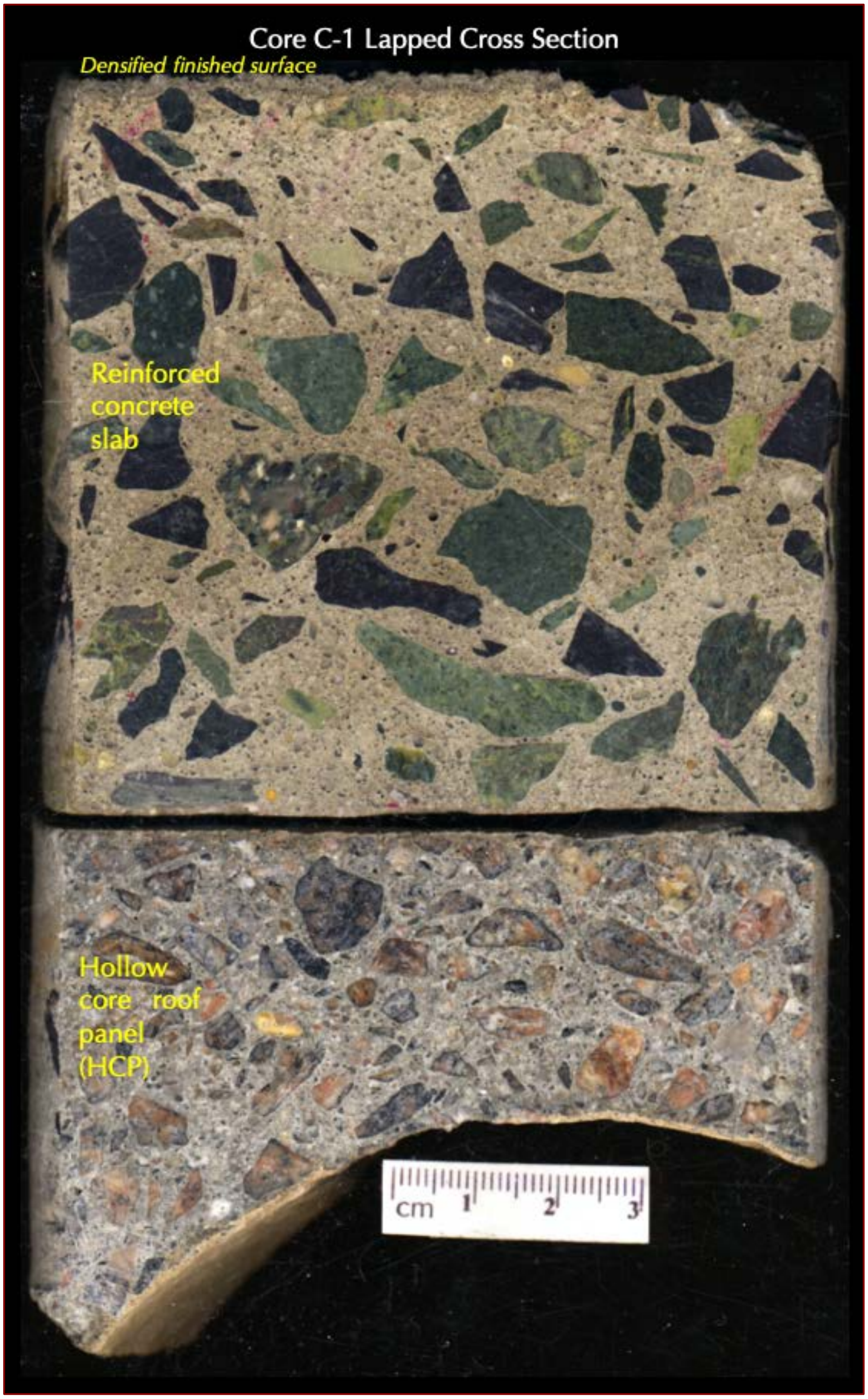

Figure 12: A second lapped cross section of Core C-1 showing: (a) the reinforced concrete slab (RCS) at the top, completely de-bonded from the hollow core roof panel (HCP) at the bottom; (b) crushed volcanic stone coarse aggregate of 1 in. (25 mm) nominal size in RCS as opposed to crushed granite coarse aggregate of $^{1}/_{2}$ in. (12.5 mm) nominal size in HCP; (c) medium beige color tone of paste in RCS as opposed to darker gray paste in HCP; (d) densified finished surface of RCS at the top $^{1}/_{8}$ in.; (e) relatively better grading of crushed granite coarse aggregate in HCP as opposed to crushed volcanic rock coarse aggregate in RCS; (f) overall dense and well-consolidated natures of RCS and HCP concretes; and (g) relatively clear separation of RCS from HCP with no trace of one adhered to the other.

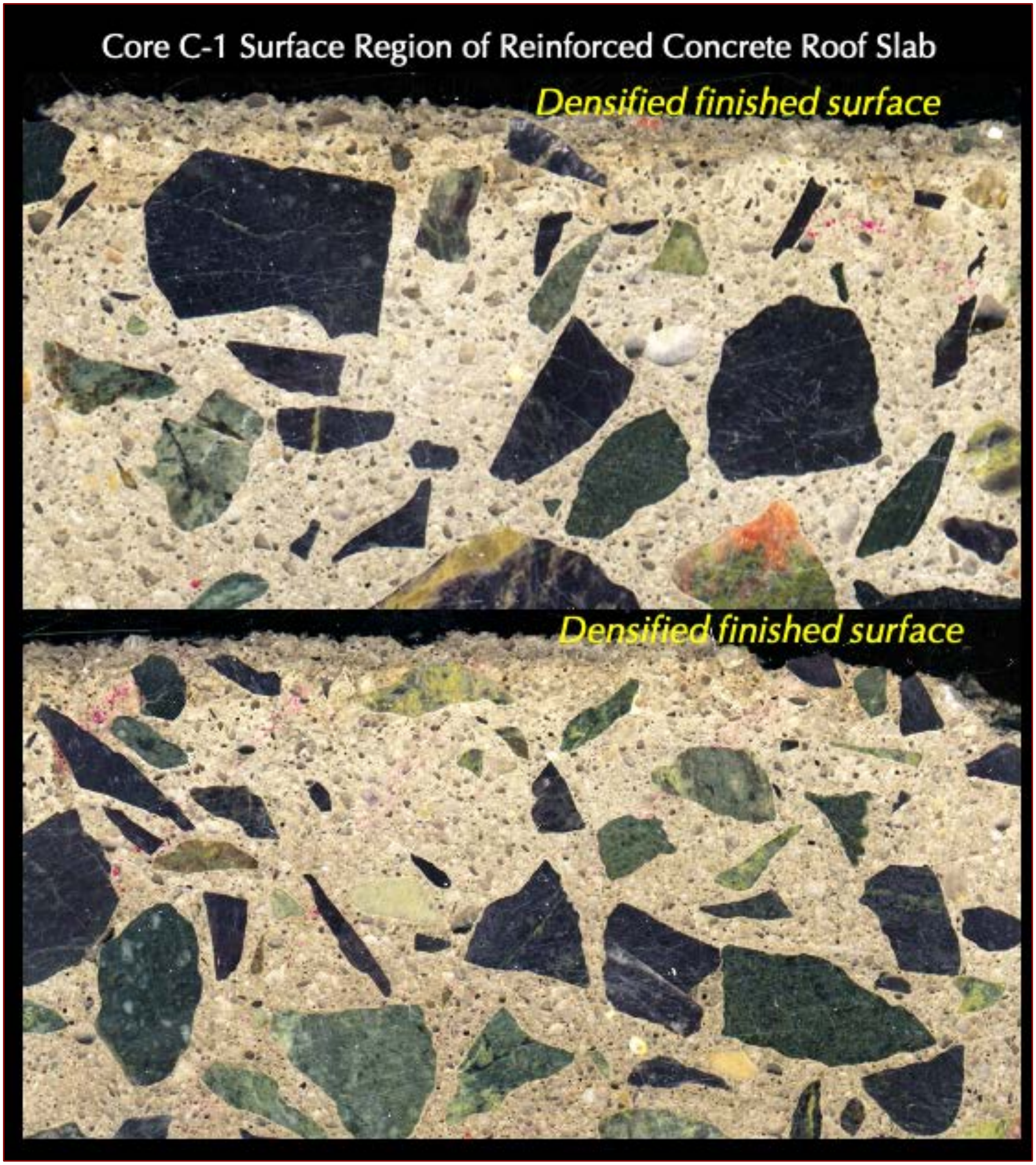

Figure 13: Lapped cross section of reinforced concrete roof top slab (RCS) portion of Core C-1 showing crushed volcanic stone coarse aggregate of 1 in. (25 mm) nominal size which are dense, hard, medium greenish-gray to black, angular, equidimensional to elongated, sound, well-graded, and well-distributed. Notice the darker gay densified finished surface at the top $^{1}/_{8}$ in. due to finishing-induced densification of the surface.

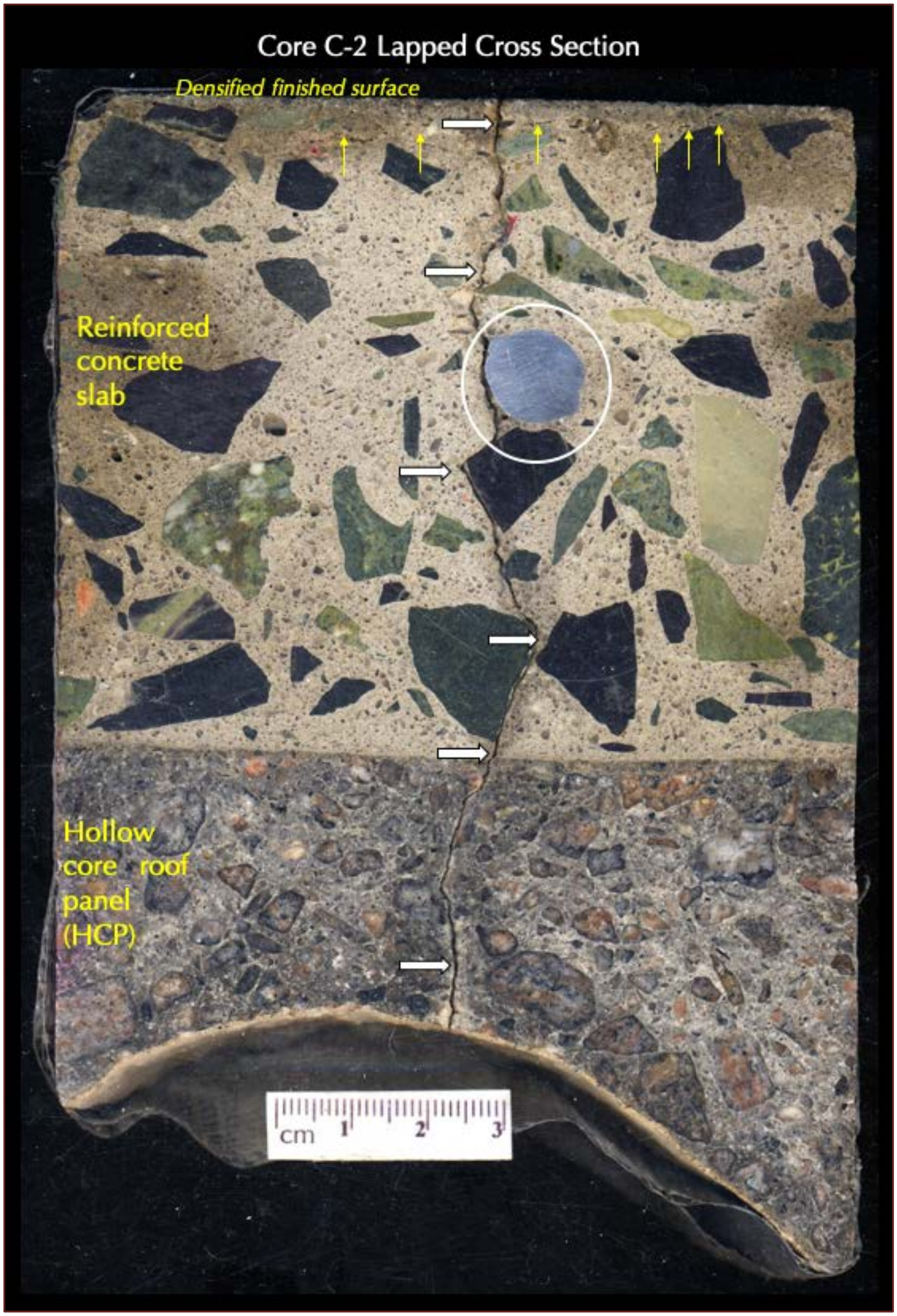

Figure 14: Lapped cross section of Core C-2 showing: (a) the reinforced concrete slab (RCS) at the top, well-bonded to the hollow core roof panel (HCP) at the bottom; (b) crushed volcanic stone coarse aggregate of 1 in. (25 mm) nominal size in RCS as opposed to crushed granite coarse aggregate of $^1/_2$ in. (12.5 mm) nominal size in HCP; (c) medium beige color tone of paste in RCS as opposed to darker gray paste in HCP; (d) densified finished surface of RCS at the top $^1/_8$ in., which has developed short, elongated gaps or separations as incipient delaminations (marked with fine vertical arrows) from the main body; (e) relatively better grading of crushed granite coarse aggregate in HCP as opposed to crushed volcanic rock coarse aggregate in RCS; (f) overall dense and well-consolidated natures of RCS and HCP concretes; and (g) a long continuous vertical crack transected through both RCS and HCP components and circumscribed the reinforcing steel at the mid-depth location of RCS.

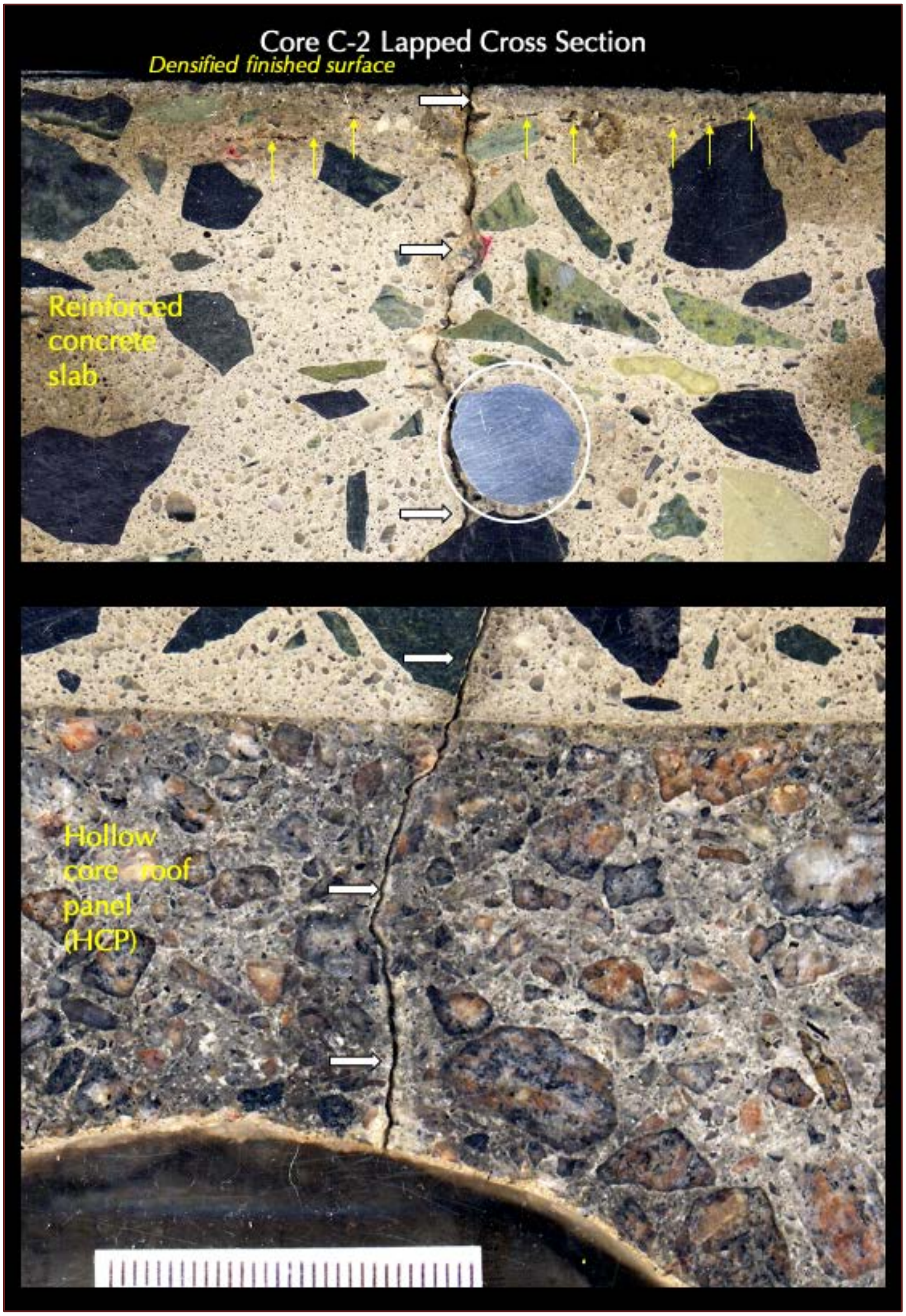

Figure 15: Lapped cross section of Core C-2 showing: (a) the reinforced concrete slab (RCS) at the top, well-bonded to the hollow core roof panel (HCP) at the bottom; (b) crushed volcanic stone coarse aggregate of 1 in. (25 mm) nominal size in RCS, as opposed to crushed granite coarse aggregate of $^1/_2$ in. (12.5 mm) nominal size in HCP; (c) medium beige color tone of paste in RCS as opposed to darker gray paste in HCP; (d) densified finished surface of RCS at the top $^1/_8$ in., which has developed short, elongated gaps or separations as incipient delaminations (marked with fine vertical arrows) from the main body; (e) relatively better grading of crushed granite coarse aggregate in HCP as opposed to crushed volcanic rock coarse aggregate in RCS; (f) overall dense and well-consolidated natures of RCS and HCP concretes; and (g) a long continuous vertical crack transected through both RCS and HCP components and circumscribed the reinforcing steel at the mid-depth location of RCS.

Figure 16: Lapped cross section of Core C-2 showing: (a) the reinforced concrete slab (RCS) at the top, well-bonded to the hollow core roof panel (HCP) at the bottom; (b) crushed volcanic stone coarse aggregate of 1 in. (25 mm) nominal size in RCS as opposed to crushed granite coarse aggregate of $^{1}/_{2}$ in. (12.5 mm) nominal size in HCP; (c) medium beige color tone of paste in RCS as opposed to darker gray paste in HCP; (d) densified finished surface of RCS at the top $^{1}/_{8}$ in., which developed short, elongated gaps or separations as incipient delaminations (marked with fine vertical arrows) from the main body; (e) relatively better grading of crushed granite coarse aggregate in HCP as opposed to crushed volcanic rock coarse aggregate in RCS; (f) overall dense and well-consolidated natures of RCS and HCP concretes; and (g) a long continuous vertical crack transected through both RCS and HCP components and circumscribed the reinforcing steel at the mid-depth location of RCS.

Figure 17: Lapped cross section of reinforced concrete roof top slab (RCS) portion of Core C-2 showing crushed volcanic stone coarse aggregate of 1 in. (25 mm) nominal size which are dense, hard, medium greenish-gray to black, angular, equidimensional to elongated, sound, well-graded, and well-distributed. Notice the darker gray densified finished surface at the top $^{1}/_{8}$ in. due to finishing-induced densification of the surface.

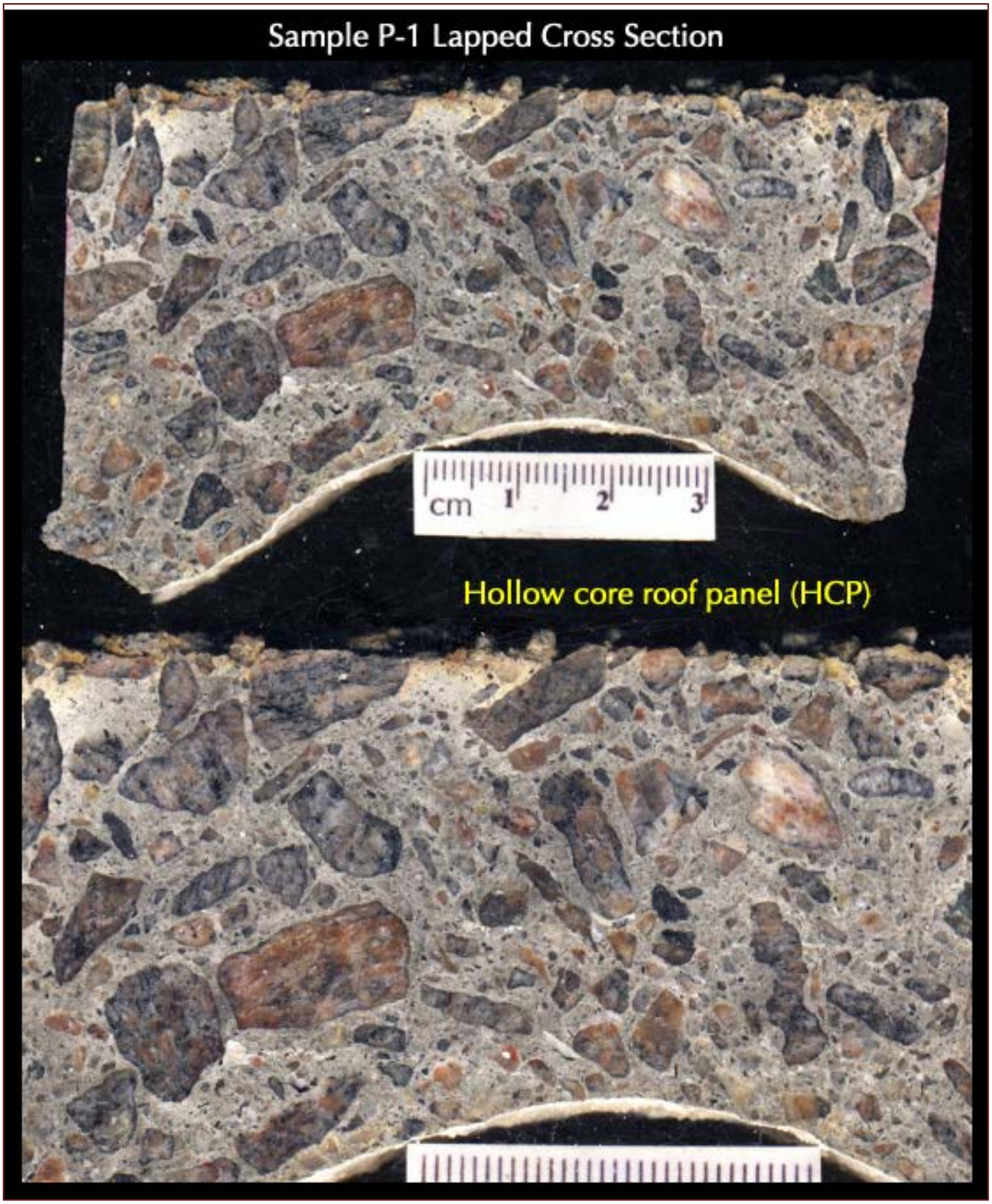

Figure 18: Lapped cross section of hollow core panel (HCP) in P-1 showing: (a) crushed granite coarse aggregate of $^1/_2$ in. (12.5 mm) nominal size; (c) dark gray paste in HCP; (d) light beige discolored altered surface at the weathered leached, carbonated end of HCP at the top edge of photos where aggregate particles are exposed relative to paste; (c) relatively sound condition of panel towards the opposite, i.e., concave end; (d) lack of air entrainment, non-air-entrained nature of HCP; and (e) relatively sound visually crack-free condition of the interior of HCP.

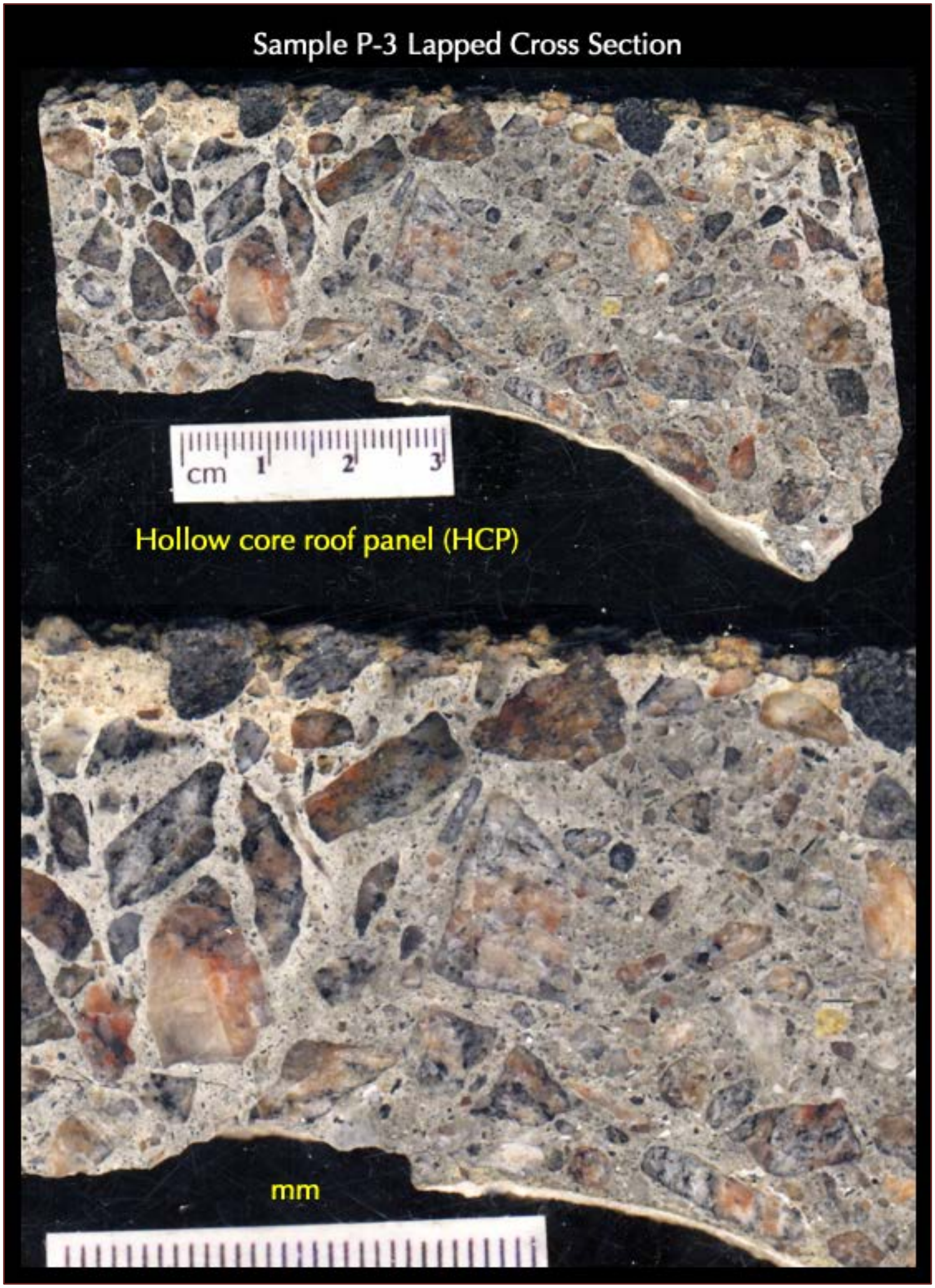

Figure 19: Lapped cross section of hollow core panel (HCP) in P-3 showing: (a) crushed granite coarse aggregate of $^{1}/_{2}$ in. (12.5 mm) nominal size; (c) dark gray paste in HCP; (d) light beige discolored altered surface at the weathered leached, carbonated end of HCP at the top edge of photos where aggregate particles are exposed relative to paste; (c) relatively sound condition of panel towards the opposite, i.e., concave end; (d) lack of air entrainment, non-air-entrained nature of HCP; and (e) relatively sound visually crack-free condition of the interior of HCP.

SAW-CUT SECTIONS AND DEPTHS OF CARBONATION

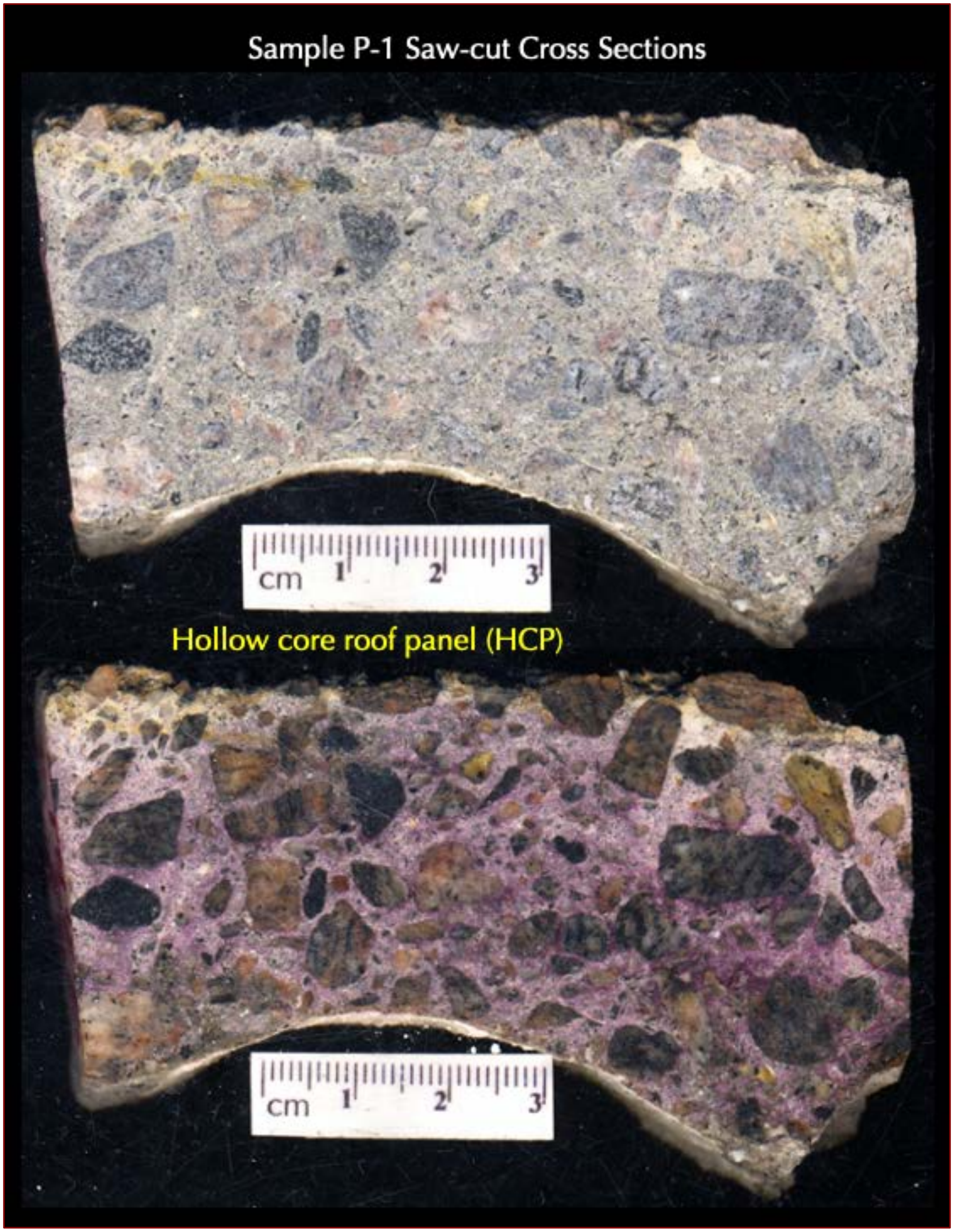

Figure 20: Saw-cut cross section of hollow core panel (HCP) in P-1 before (top) and after (bottom) treatment with phenolphthalein alcoholic solutions to highlight the carbonated paste at the top 5 to 10 mm of the altered weathered brown surface where aggregate particles are exposed relative to paste, and overall non-carbonated interior body due to pinkish discoloration of paste after the treatment.

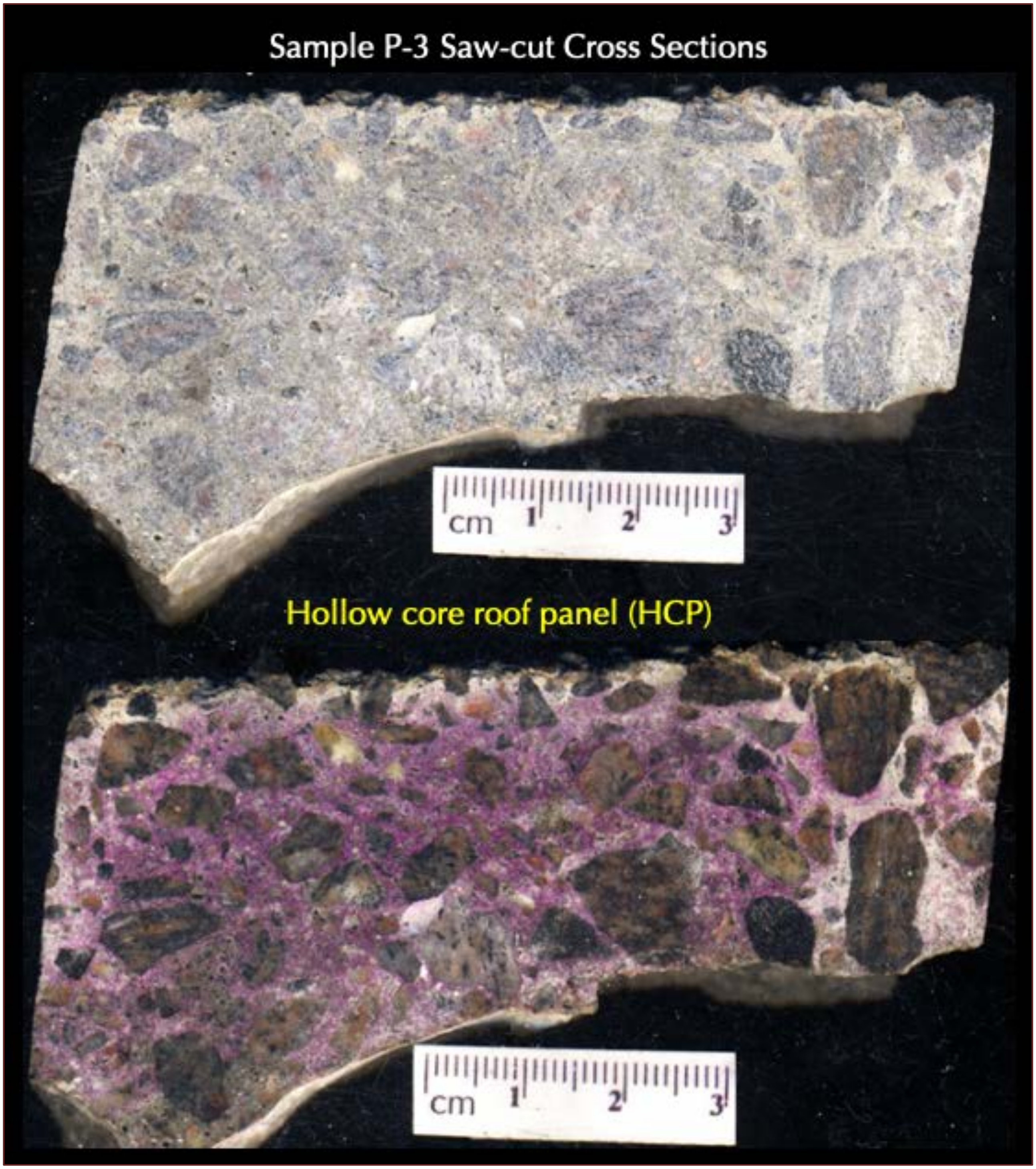

Figure 21: Saw-cut cross section of hollow core panel (HCP) in P-3 before (top) and after (bottom) treatment with phenolphthalein alcoholic solutions to highlight the carbonated paste at the top 5 to 10 mm of the altered weathered brown surface where aggregate particles are exposed relative to paste, and overall non-carbonated interior body due to pinkish discoloration of paste after the treatment.

MICROGRAPHS OF LAPPED CROSS SECTION

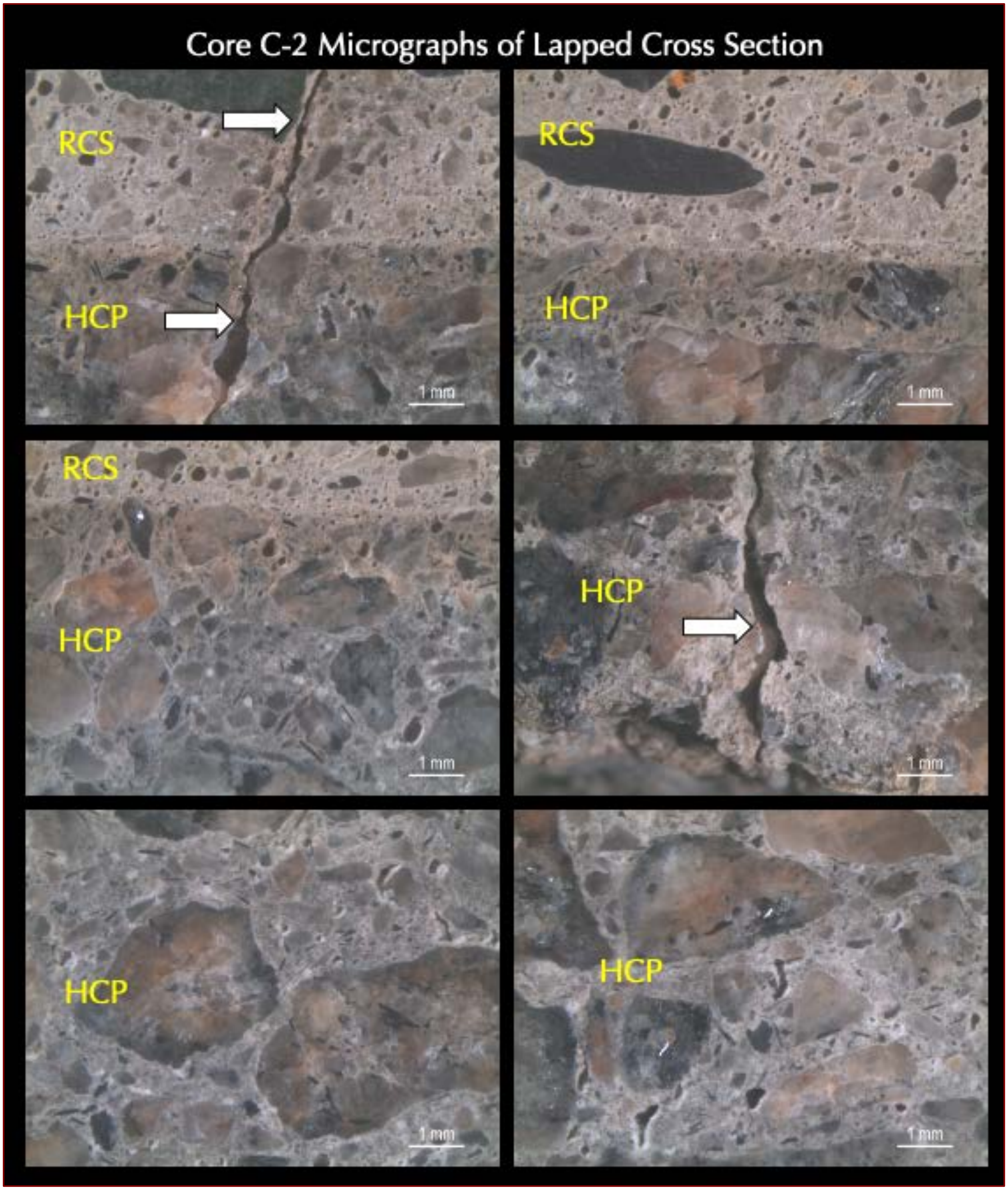

Figure 22: Micrographs of lapped cross section of Core C-2 showing: (a) the excessively air-entrained reinforced concrete slab (RCS) as opposed to non-air-entrained hollow core panel (HCP) with a good bond between the two components; and (b) a vertical crack trasected through both RCS and HCP components.

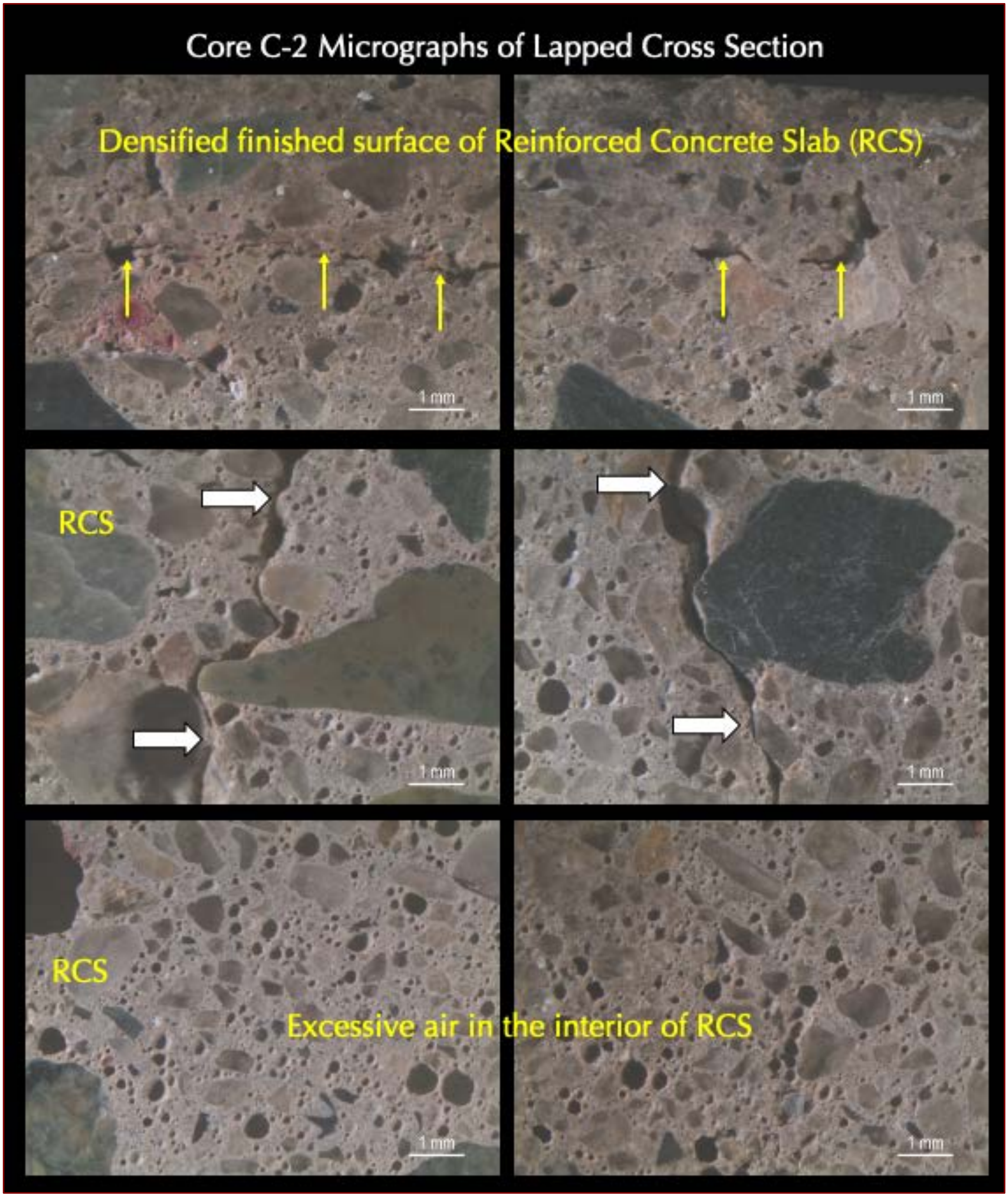

Figure 23: Micrographs of lapped cross section of Core C-2 showing: (a) the excessively air-entrained reinforced concrete slab (RCS), and, (b) lack of air voids at the top $^{1}/_{8}$ in. due to finishing-induced densification of an excessively air-entrained concrete, which has developed short, discontinuous, elongated gaps or separations as incipient delaminations, which are marked as yellow arrows in the top two photos. Notice the main vertical crack transected through the RCS.

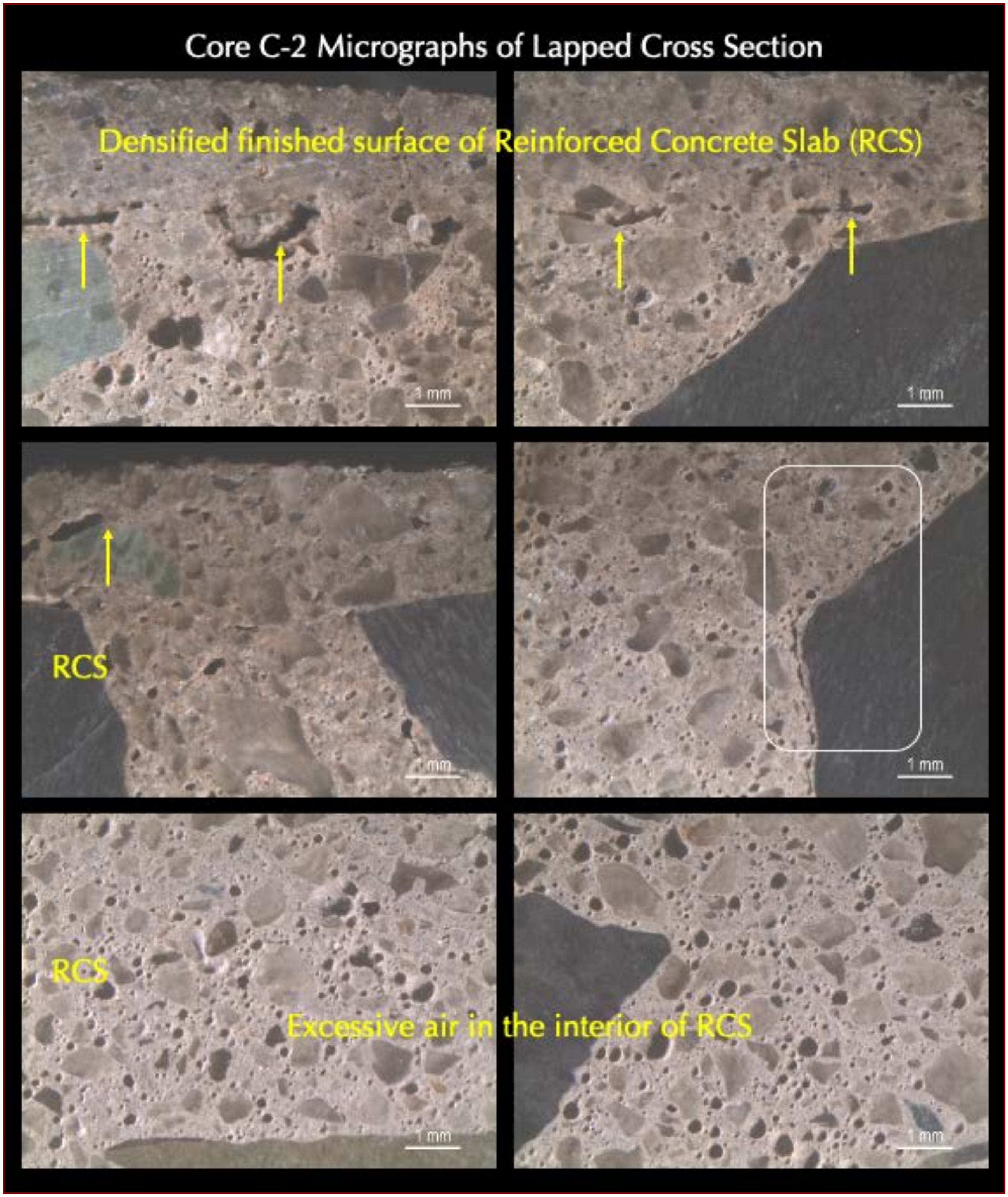

Figure 24: Micrographs of lapped cross section of Core C-2 showing: (a) the excessively air-entrained reinforced concrete slab (RCS), and, (b) lack of air voids at the top $^1/_8$ in. due to finishing-induced densification of an excessively air-entrained concrete, which has developed short, discontinuous, elongated gaps or separations as incipient delaminations, which are marked as yellow arrows in the top two and middle left photos. Notice clustering of air voids at aggregate-paste interfaces (boxed in middle right photo) due to excessive air entrainment in the RCS.

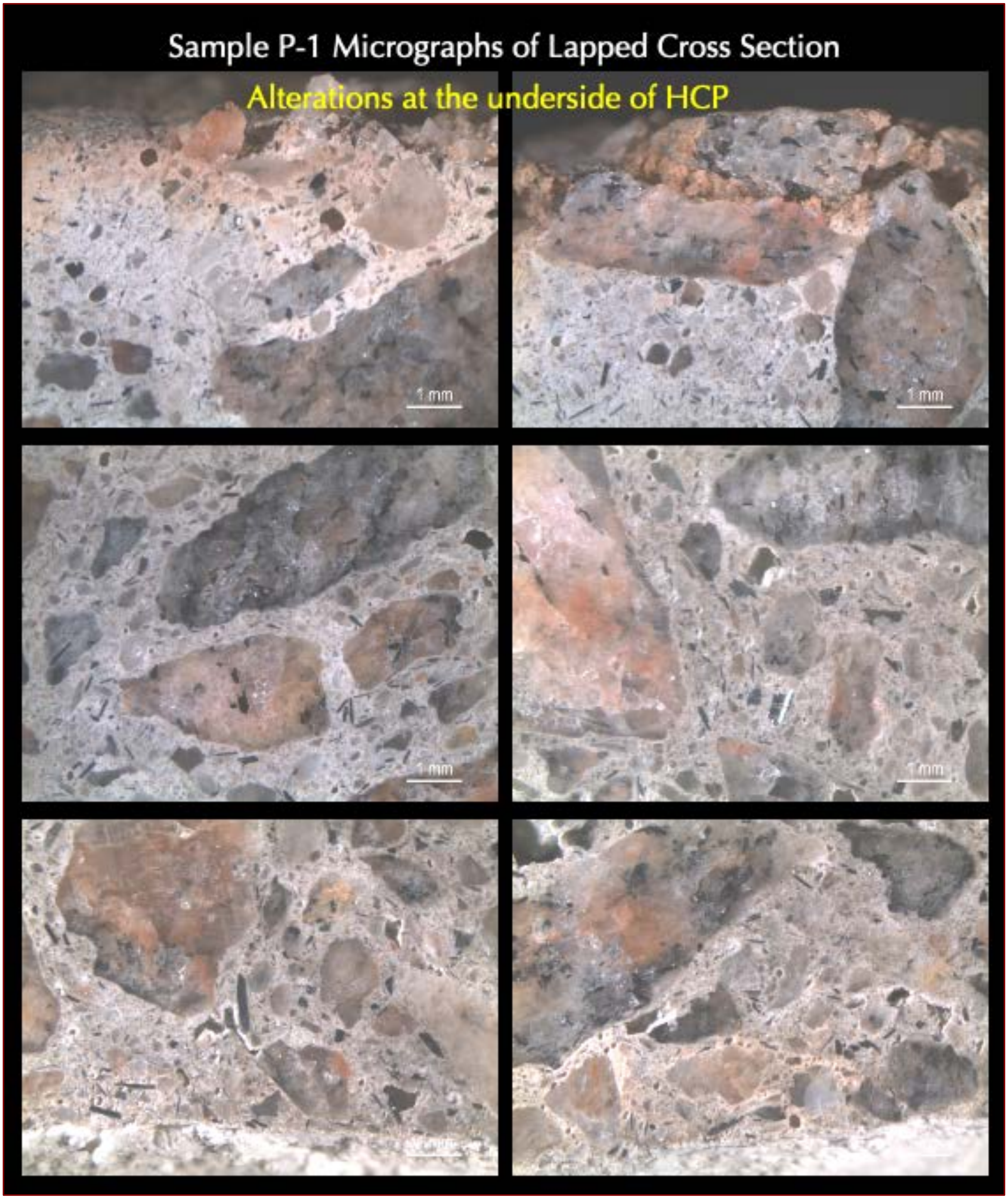

Figure 25: Micrographs of lapped cross section of hollow core panel (HCP) in P-1 showing: (a) altered, discolored light beige cabronated paste at the top 5 to 10 mm of weathered brown surface of HCP in the top two photos where aggregate particles are exposed relative to paste, and (b) interior non-air-entrained concrete in the middle and bottom row photos.

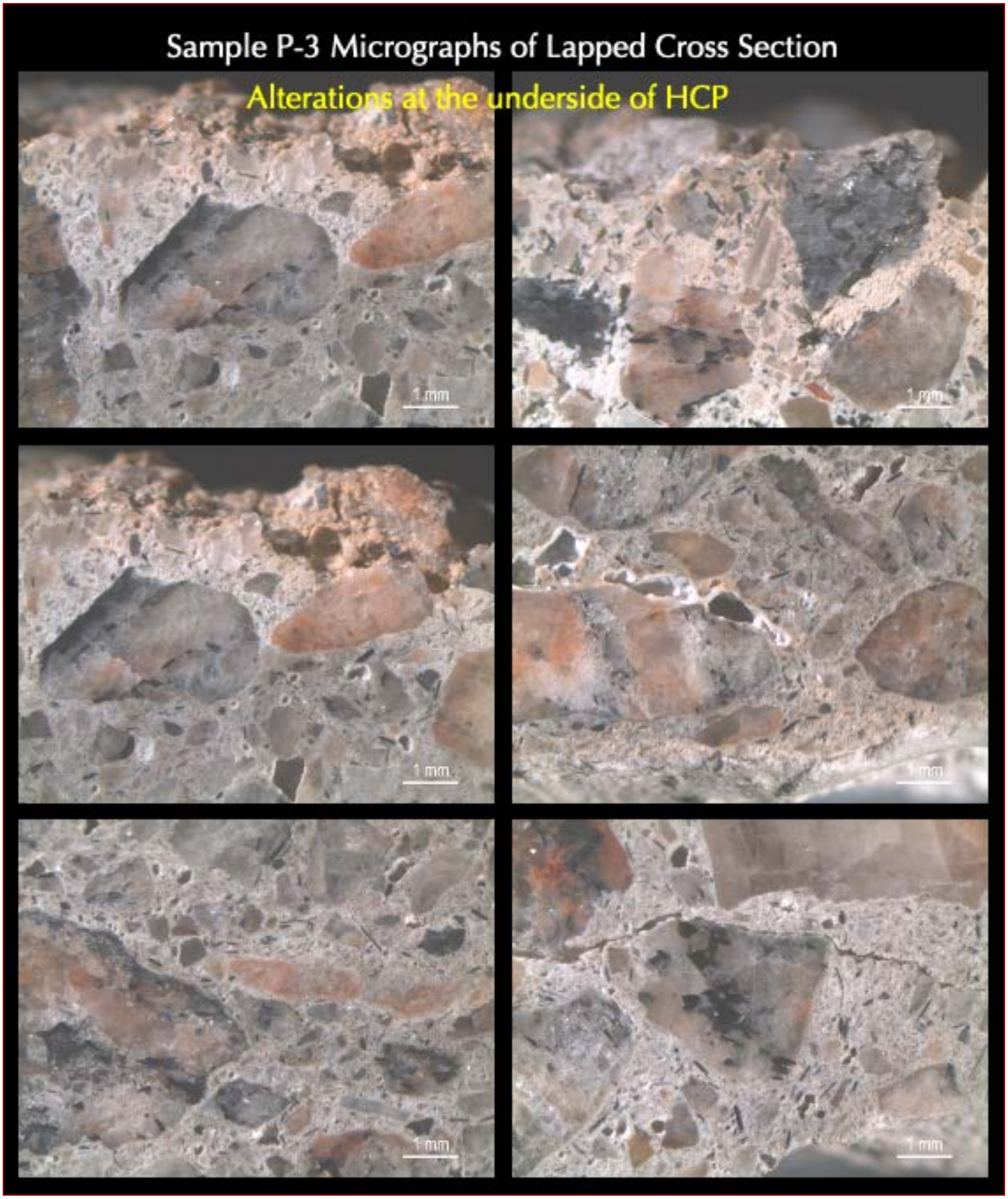

Figure 26: Micrographs of lapped cross section of hollow core panel (HCP) in P-3 showing: (a) altered, discolored light beige carbonated paste at the top 5 to 10 mm of weathered brown surface of HCP in the top two photos, where aggregate particles are exposed relative to paste, and (b) interior non-air-entrained concrete in the middle and bottom row photos. Notice fine horizontal cracks beneath the altered zone in the bottom right photo. Notice white secondary ettringite deposits lining the walls of entrapped air voids in the top and middle right photos.

THIN SECTIONS

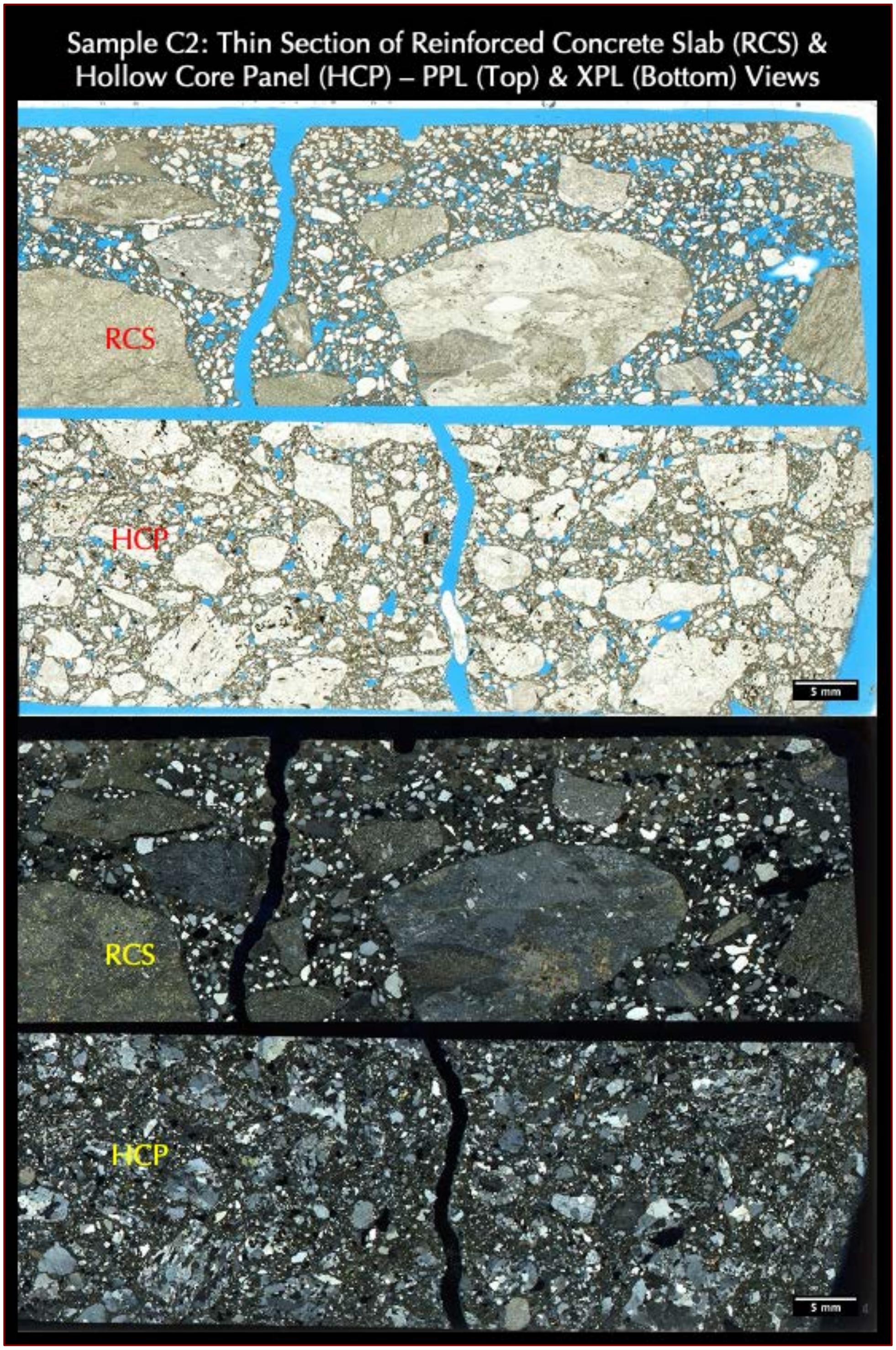

Figure 27: Blue dye-mixed epoxy-impregnated thin section of Core C-2 in plane polarized light (PPL) at the top and corresponding crossed-polarized light (XPL) mode at the bottom showing: (a) the crushed volcanic stone coarse aggregate particles in RCS as opposed to finer sized crushed granite coarse aggregate in HCP; (b) crushed silica sand fine aggregate in both RCS and HCP; (c) excesively air-entrained RCS as opposed to non-air-entrained HCP where air voids are highlighted in blue epoxy in PPL, and (c) overall dense, non-carbonated interiors of both RCS and HCP which are evident in both PPL and XPL images.

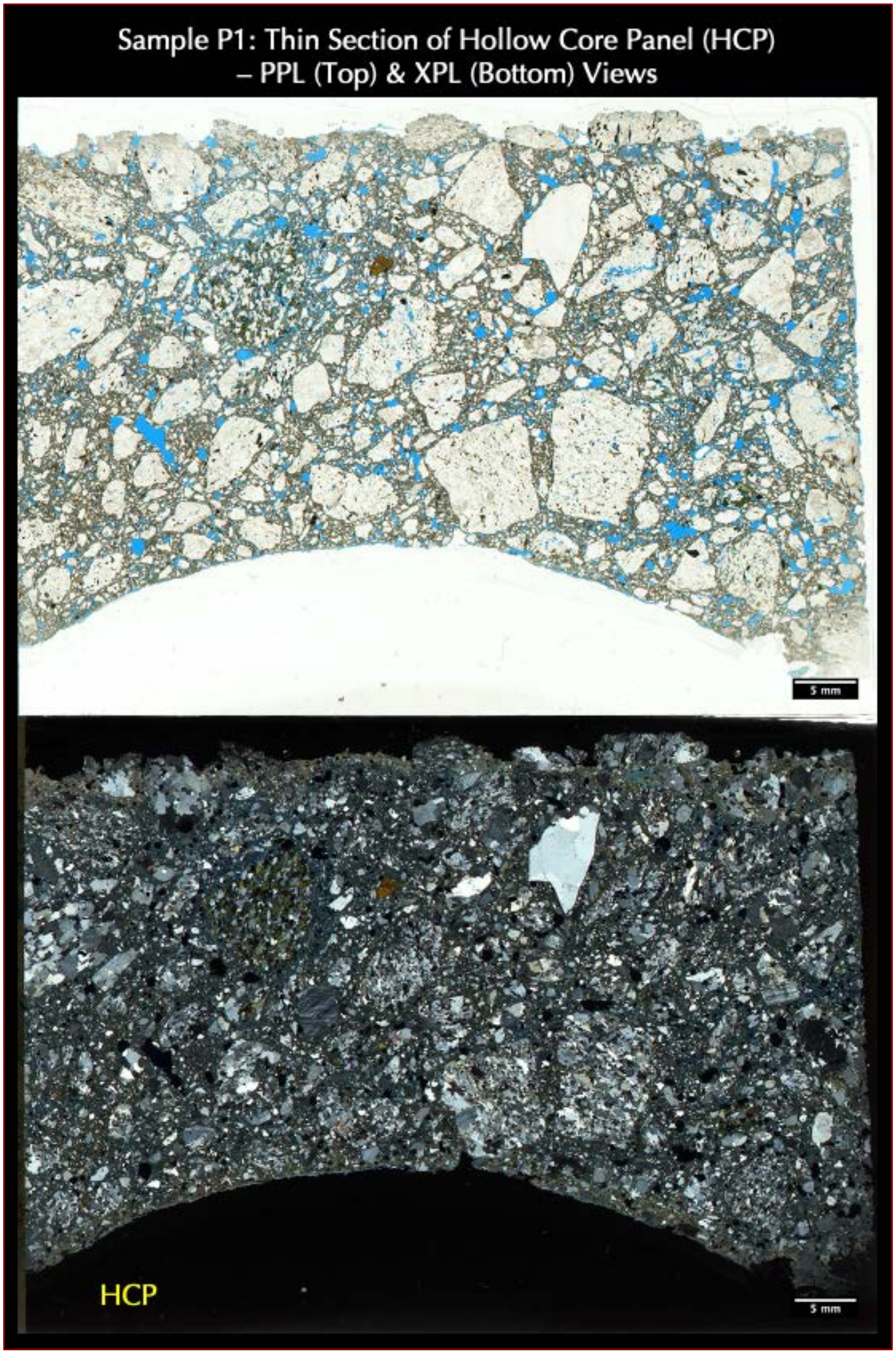

Figure 28: Blue dye-mixed epoxy-impregnated thin section of P-1 in plane polarized light (PPL) at the top and corresponding crossed-polarized light (XPL) mode at the bottom showing: (a) the crushed granite coarse aggregate in HCP; (b) crushed silica sand fine aggregate in both RCS and HCP; (c) excessively air-entrained RCS as opposed to non-air-entrained HCP, where air voids are highlighted in blue epoxy in PPL, and (c) overall dense, non-carbonated interiors of both RCS and HCP, which are evident in both PPL and XPL images. Surface alterations of paste at the weathered brown surface end is not distinct in the entire image in XPL mode except some paste carbonation.

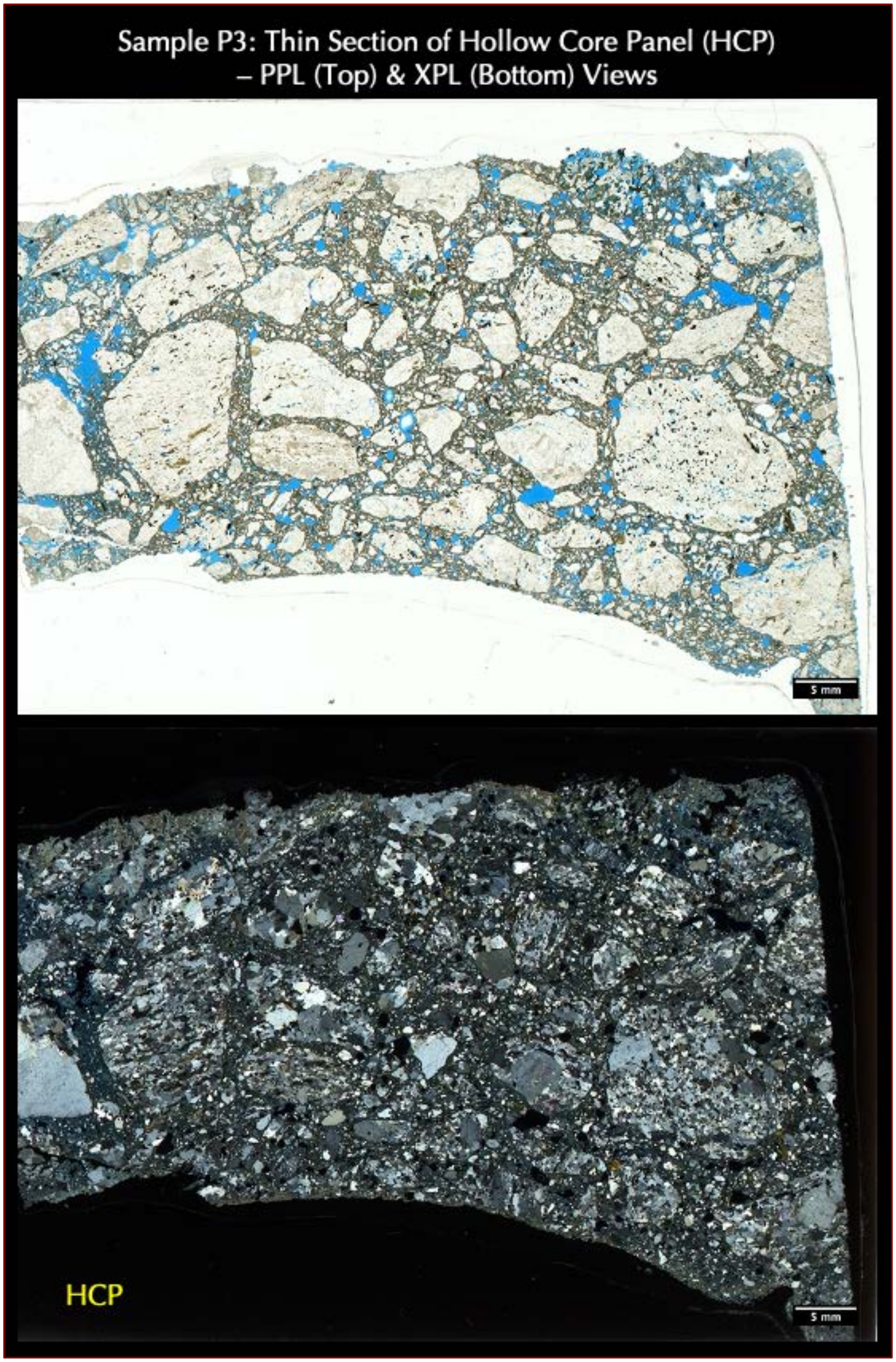

Figure 29: Blue dye-mixed epoxy-impregnated thin section of P-3 in plane polarized light (PPL) at the top and corresponding crossed-polarized light (XPL) mode at the bottom showing: (a) the crushed granite coarse aggregate in HCP; (b) crushed silica sand fine aggregate in both RCS and HCP; (c) excessively air-entrained RCS as opposed to non-air-entrained HCP, where air voids are highlighted in blue epoxy in PPL, and (c) overall dense, non-carbonated interiors of both RCS and HCP, which are evident in both PPL and XPL images. Surface alterations of paste at the weathered brown surface end is not distinct in the entire image in XPL mode except some paste carbonation.

BLACK AND WHITE CONTRAST ENHANCEMENT

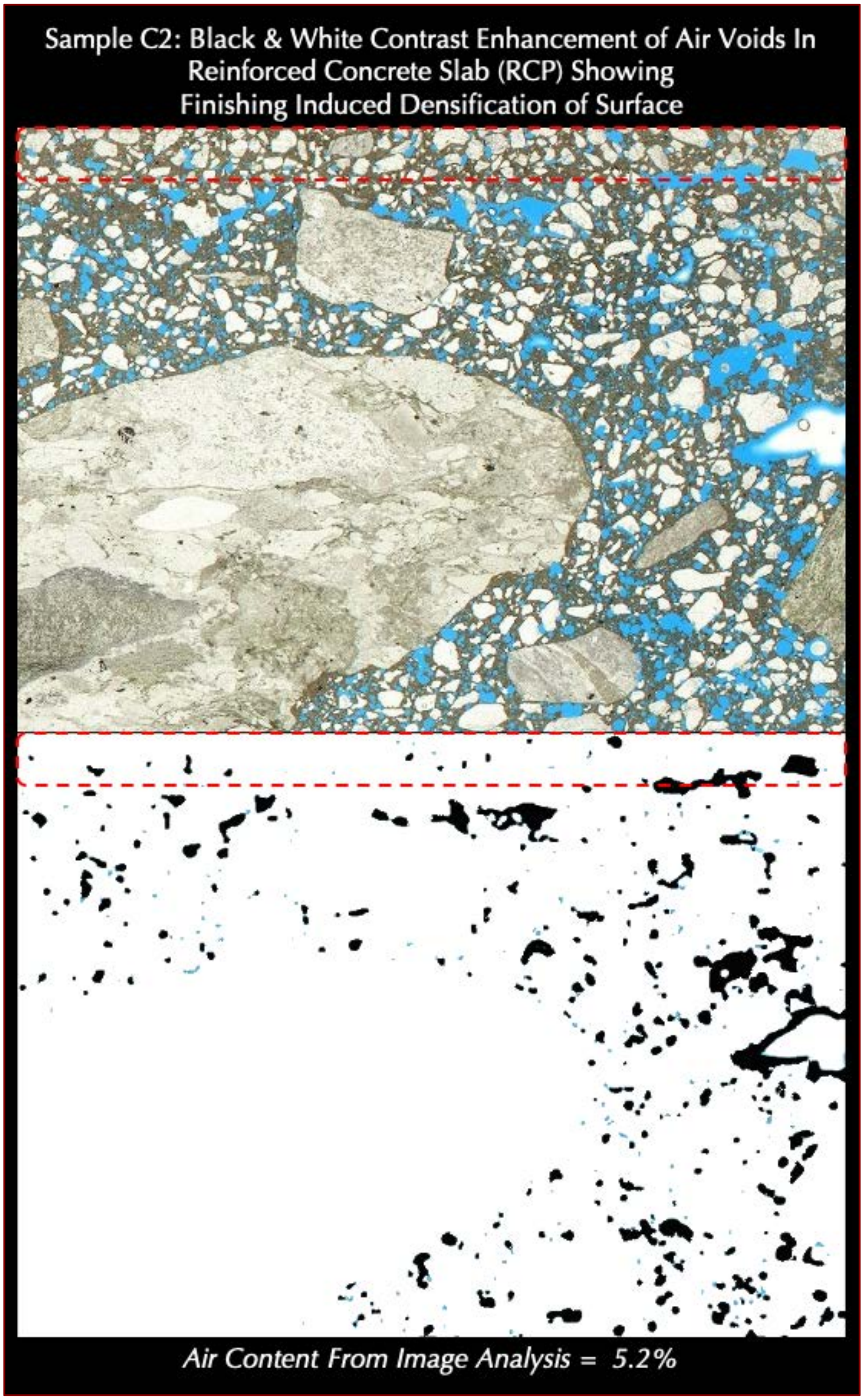

Figure 30: Black and white contrast enhancement of PPL image of RCS in Core C-2 where air voids are highlighted in blue epoxy in the top and corresponding black areas in the bottom binary image where air voids are highlighted in black against everything else in white to calculate air content of RCS as 5.2 percent by volume. The air content is lower than actually observed in the range of 10 to 12 percent (e.g., see Figures 22 and 23) due to the presence of a coarse aggregate particle covering almost 40 percent area of the image.

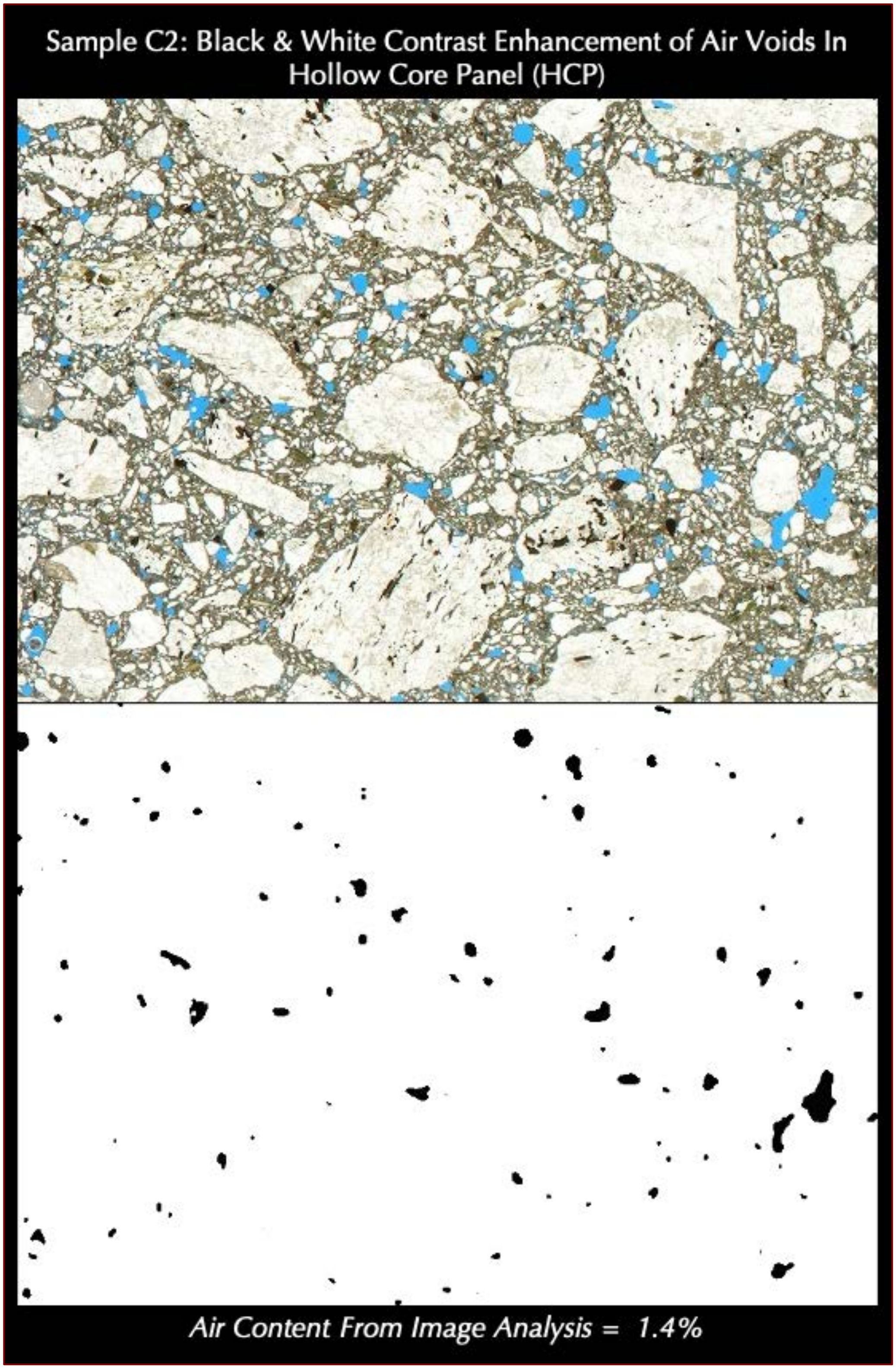

Figure 31: Black and white contrast enhancement of PPL image of HCP in Core C-2 where air voids are highlighted in blue epoxy in the top and corresponding black areas in the bottom binary image where air voids are highlighted in black against everything else in white to calculate air content of HCP as 1.4 percent by volume.

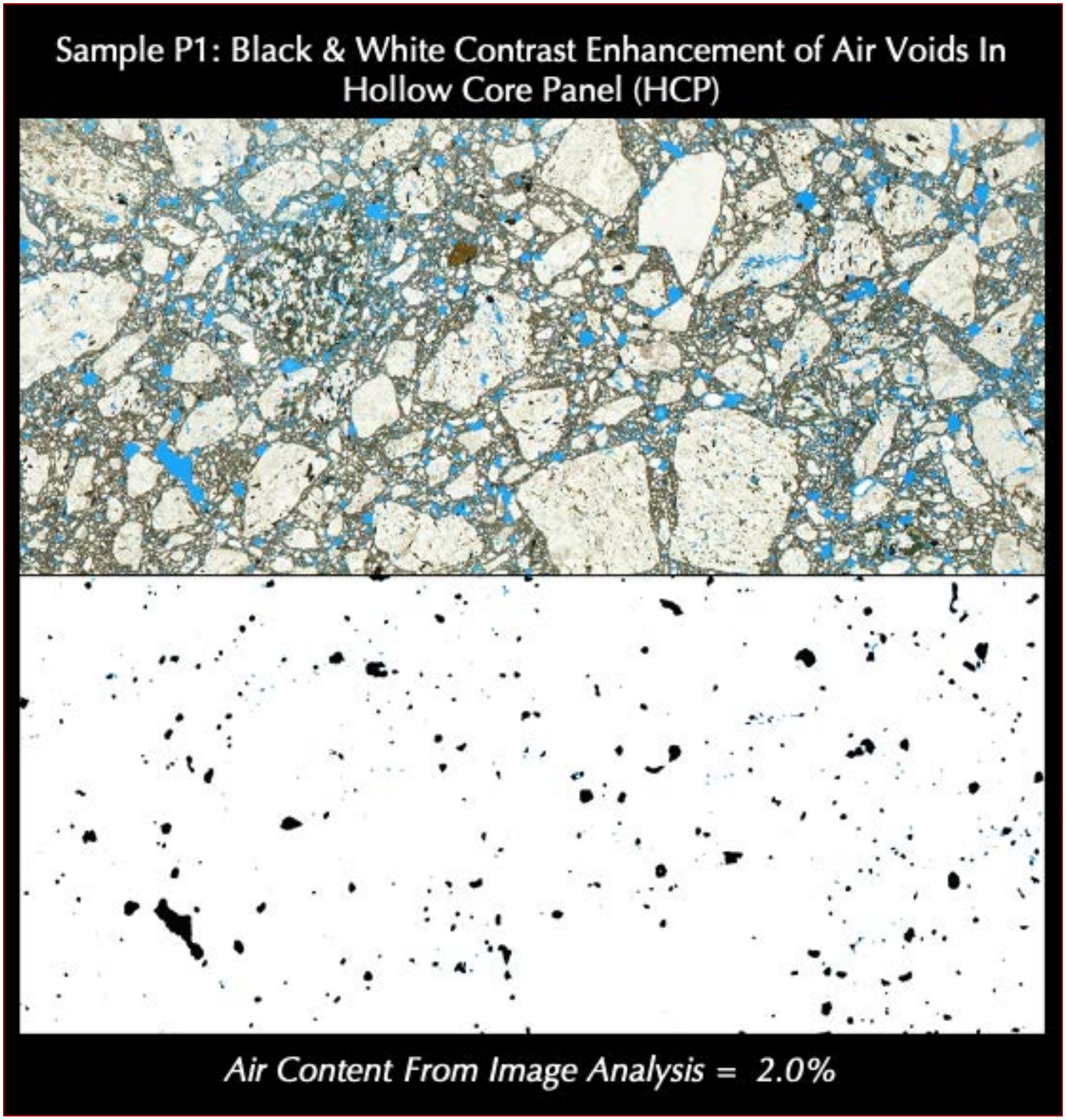

Figure 32: Black and white contrast enhancement of PPL image of HCP in P-1 where air voids are highlighted in blue epoxy in the top and corresponding black areas in the bottom binary image where air voids are highlighted in black against everything else in white to calculate air content of HCP as 2.0 percent by volume.

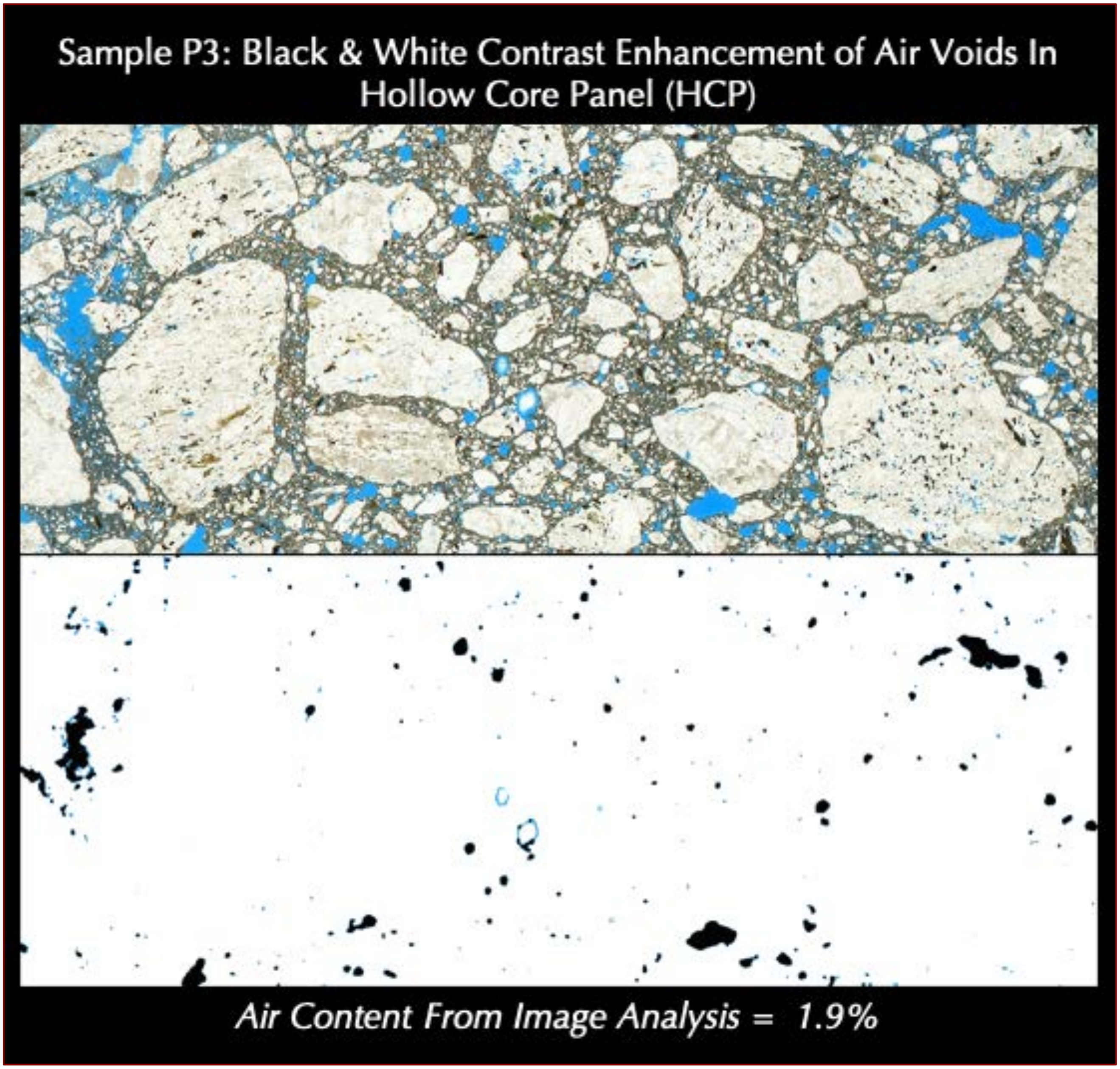

Figure 33: Black and white contrast enhancement of PPL image of HCP in P-3 where air voids are highlighted in blue epoxy in the top and corresponding black areas in the bottom binary image where air voids are highlighted in black against everything else in white to calculate air content of HCP as 1.9 percent by volume. Air contents in three HCPs in Core C-2 and in Samples P1 and P3 are calculated as 1.4%, 2.0%,and 1.9%, respectively, which are noticeably lower than the minimal air content in RCS calculated from image analysis to be 5.2% in Figure 29.

MICROGRAPHS OF THIN SECTIONS

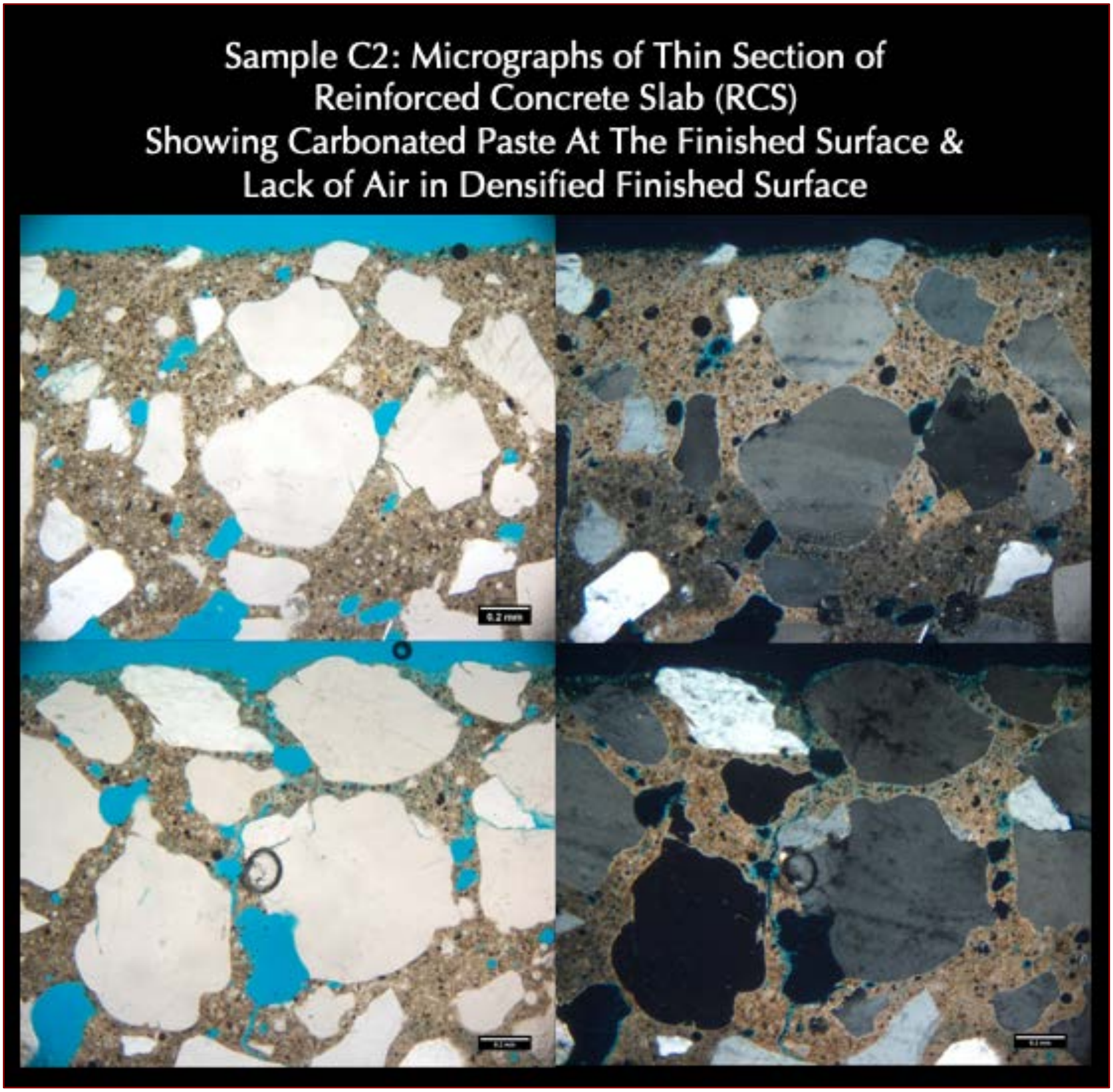

Figure 34: Micrographs of thin section of RCS in Core C-2 showing the golden yellow interference color of carbonated paste at the finished surface region in the right column photos taken in XPL mode of the corresponding PPL images in left column where finishing-induced densification of paste is also noted due to the lack of overall entrained air voids that are excessively present in the interior body. Also notice the presence of a few, fine, spherical black fly ash particles in the paste in the PPL images indicating a binary cementitious mix of major amount of Portland cement and subordinate amount of fly ash. Scale bars are 0.1 mm in length.

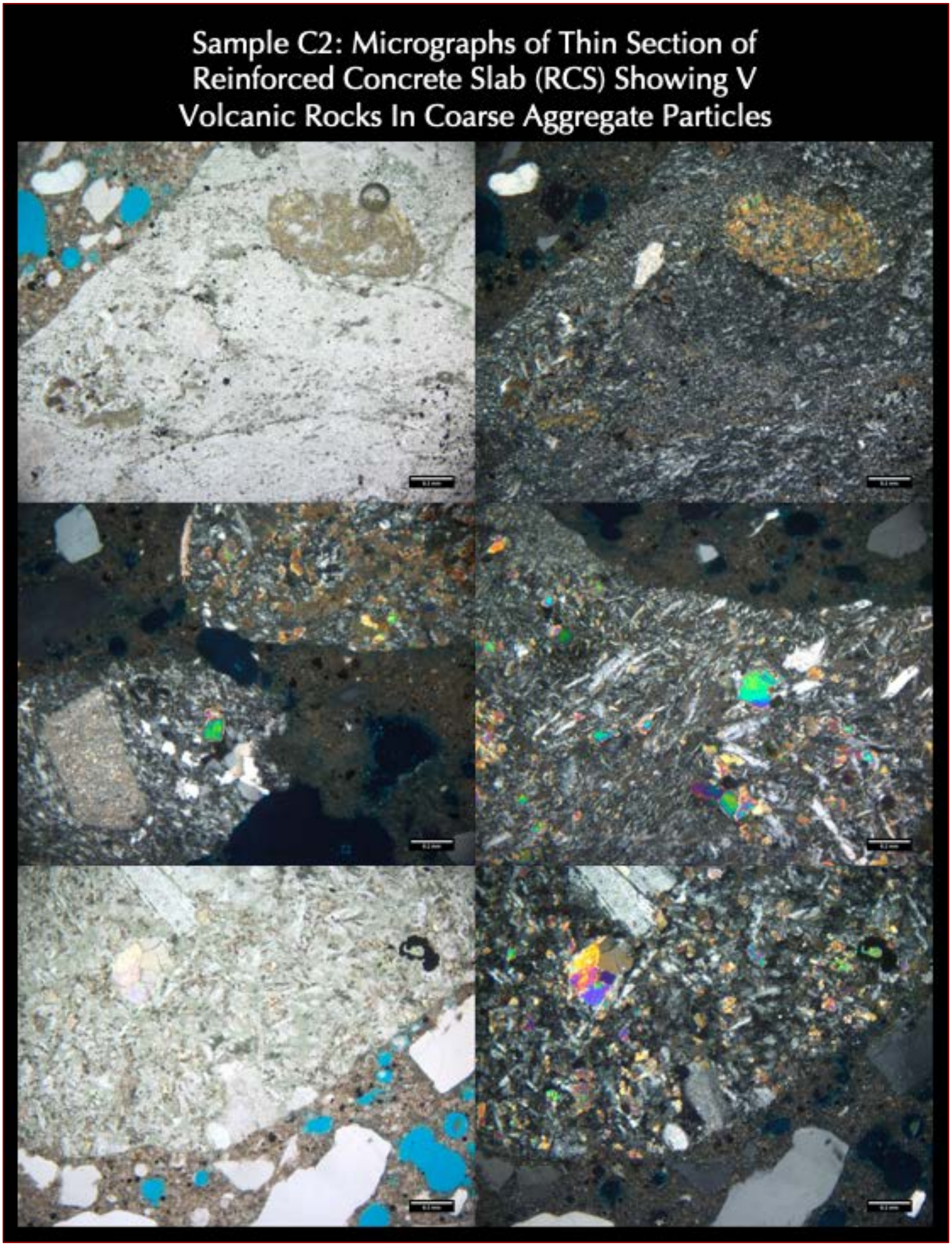

Figure 35: Micrographs of thin section of RCS in Core C-2 showing the crushed volcanic rock coarse aggregate particles consisting of basalt, and andesite particles in crushed stone and crushed silica sand fine aggregate particles. Scale bars are 0.2 mm in length.

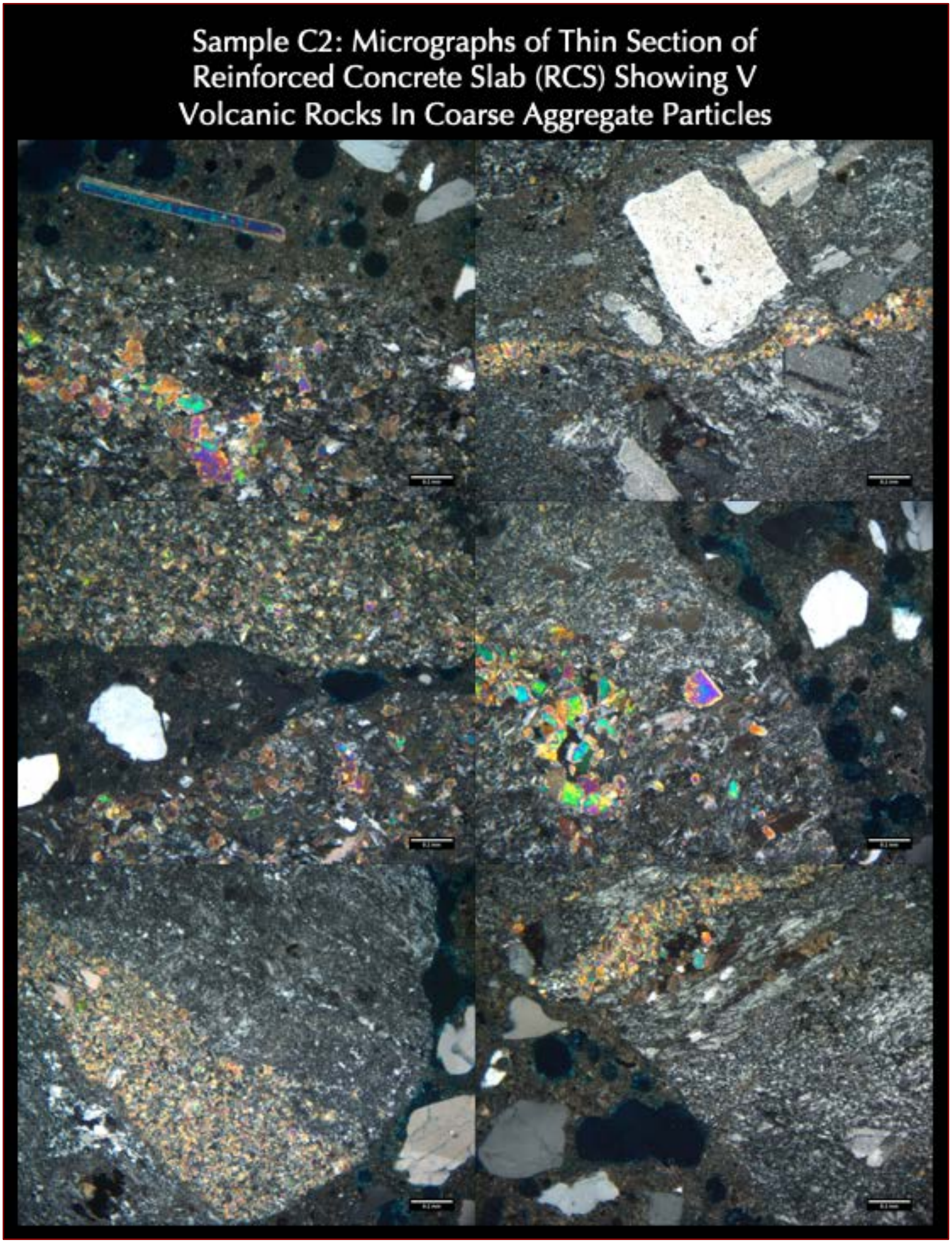

Figure 36: Micrographs of thin section of RCS in Core C-2 showing the crushed volcanic rock coarse aggregate particles consisting of basalt, and andesite particles in crushed stone and crushed silica sand fine aggregate particles. Scale bars are 0.2 mm in length.

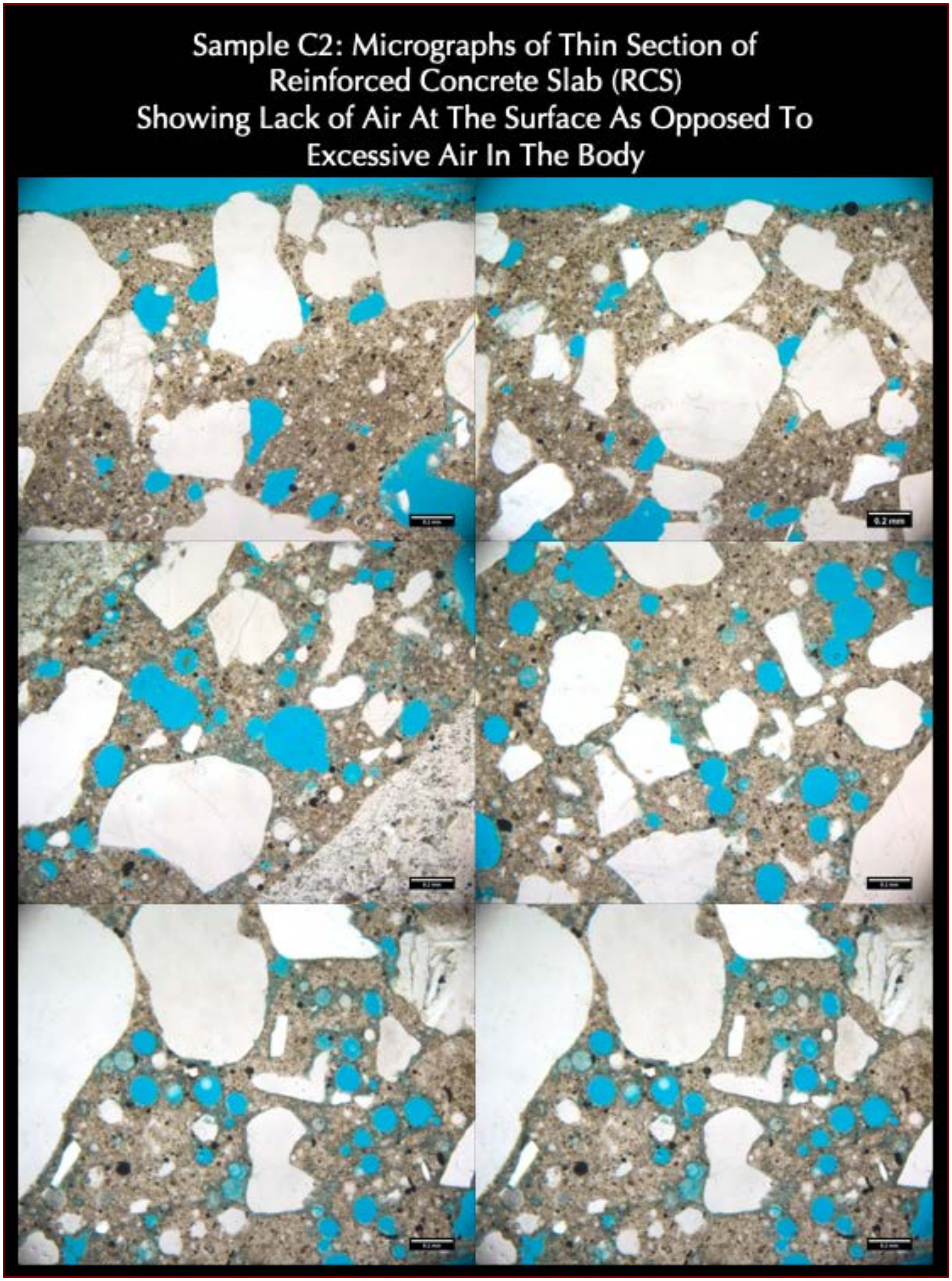

Figure 37: Micrographs of thin section of RCS in Core C-2 showing the finishing-induced loss of air voids at the top finished surface regions in the top row photos where only a few irregular-shaped air voids are highlighted in blue epoxy as opposed to excessively air-entrained fine, discrete spherical and near-spherical entrained air voids in the interior in middle and bottom row photos where spherical entrained air voids are highlighted in blue epoxy. Scale bars are 0.2 mm in length.

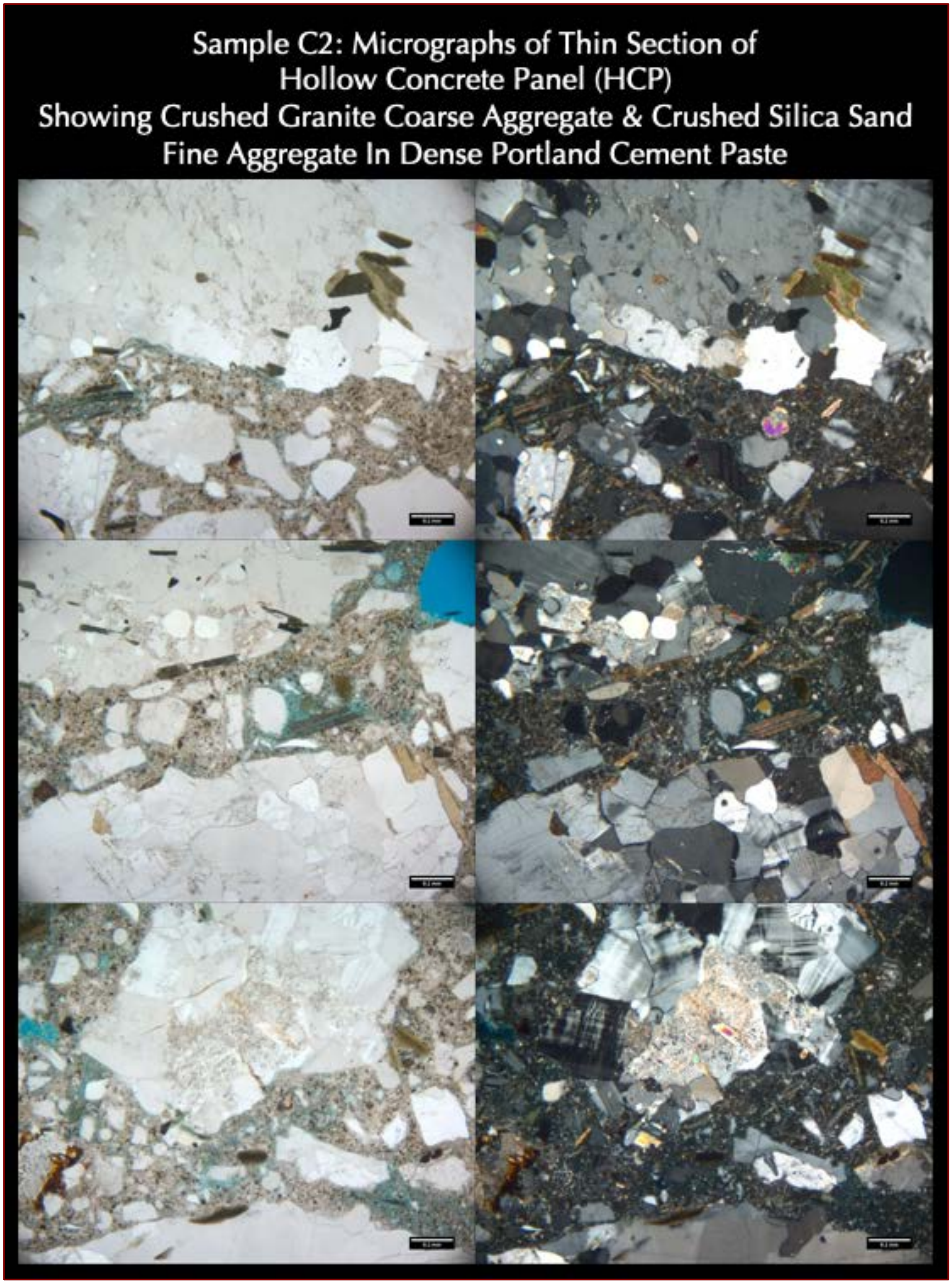

Figure 38: Micrographs of thin section of hollow core panel (HCP) component in Core C-2 showing the crushed granite coarse aggregate particles having quartz, alkali feldspar (microcline with crisscross twins, and orthoclase), and plagioclase (albite) mineralogies of granite with minor muscovite and biotite flakes, showing typical coarse-grained intergranular crystalline texture of granite, and crushed silica sand fine aggregate particles having major amounts of quartz and subordinate amounts of quartzite, granite, feldspar particles and dense interstitial Portland cement paste without any spherical particles of residual fly ash found in the RCS component. Scale bars are 0.2 mm in length.

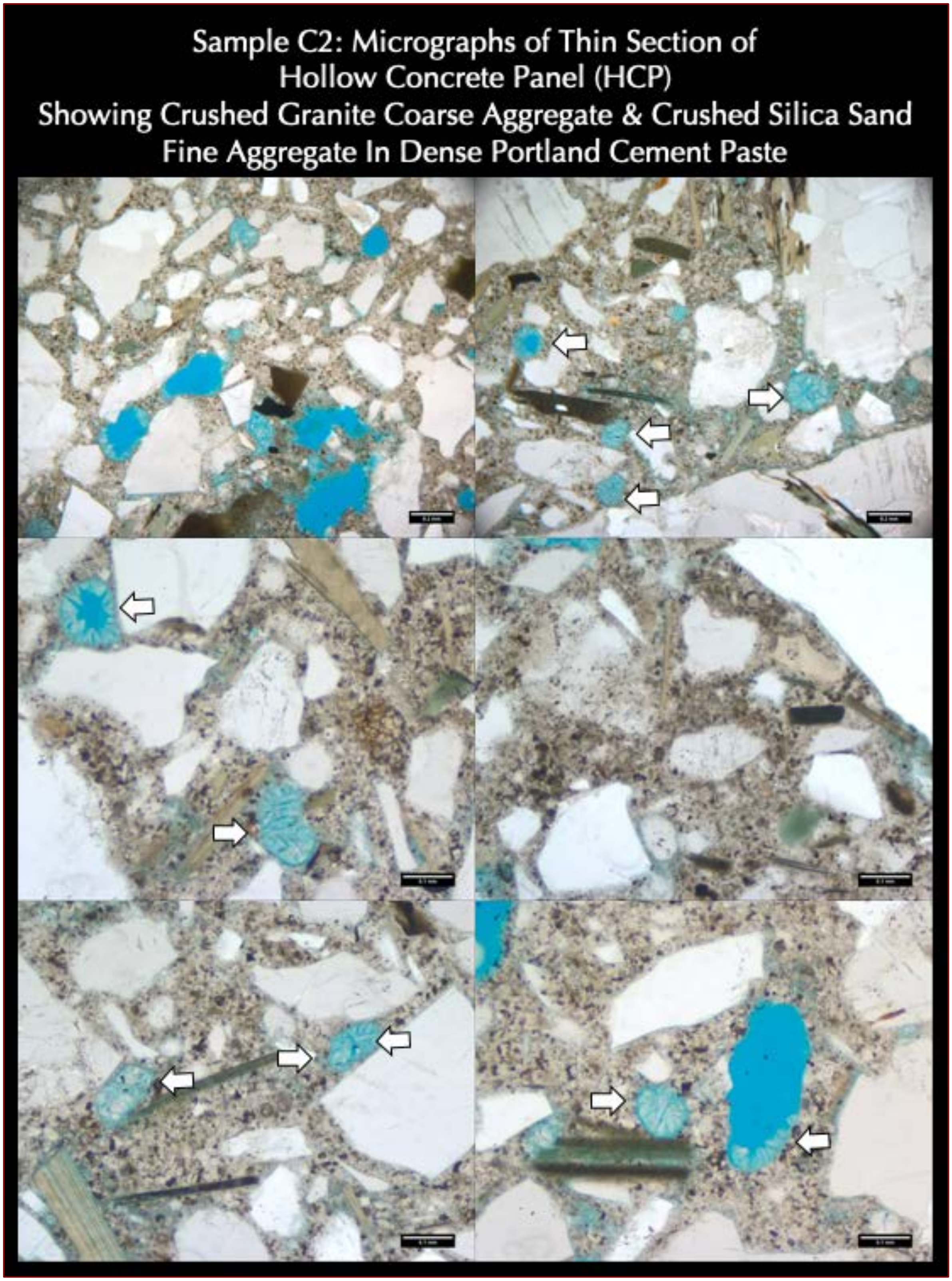

Figure 39: Micrographs of thin section of hollow core panel (HCP) component in Core C-2 showing the dense Portland cement paste between the crushed granite coarse aggregate, crushed silica sand fine aggregate, and sporadic irregular-shaped entrapped air voids many lined with fibrous secondary ettringite deposits indicating prolonged presence of moisture in HCP during service. Scale bars are 0.1 mm in length.

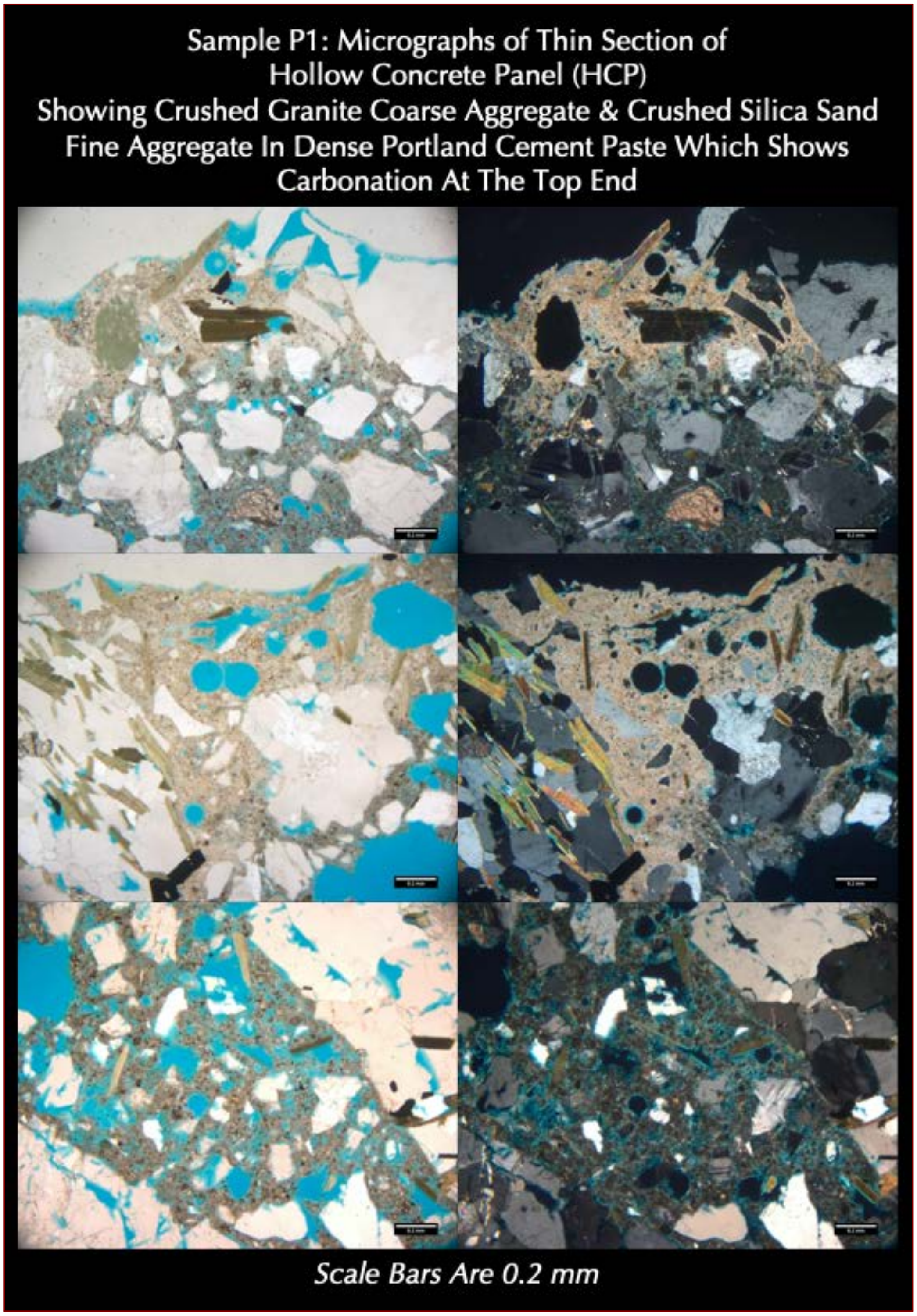

Figure 40: Micrographs of thin section of hollow core panel (HCP) in P-1 showing the crushed granite coarse aggregate particles having quartz, alkali feldspar (microcline, and orthoclase), and plagioclase (albite) mineralogies of granite with minor muscovite and biotite flakes, showing typical coarse-grained intergranular crystalline texture of granite, and crushed silica sand fine aggregate particles having major amounts of quartz and subordinate amounts of quartzite, granite, feldspar particles and dense interstitial Portland cement paste without any spherical particles of residual fly ash found in the RCS component. Notice golden yellow interference color of carbonated paste at the altered weathered brown surface of HCP that are highlighted in top and middle right XPL images.

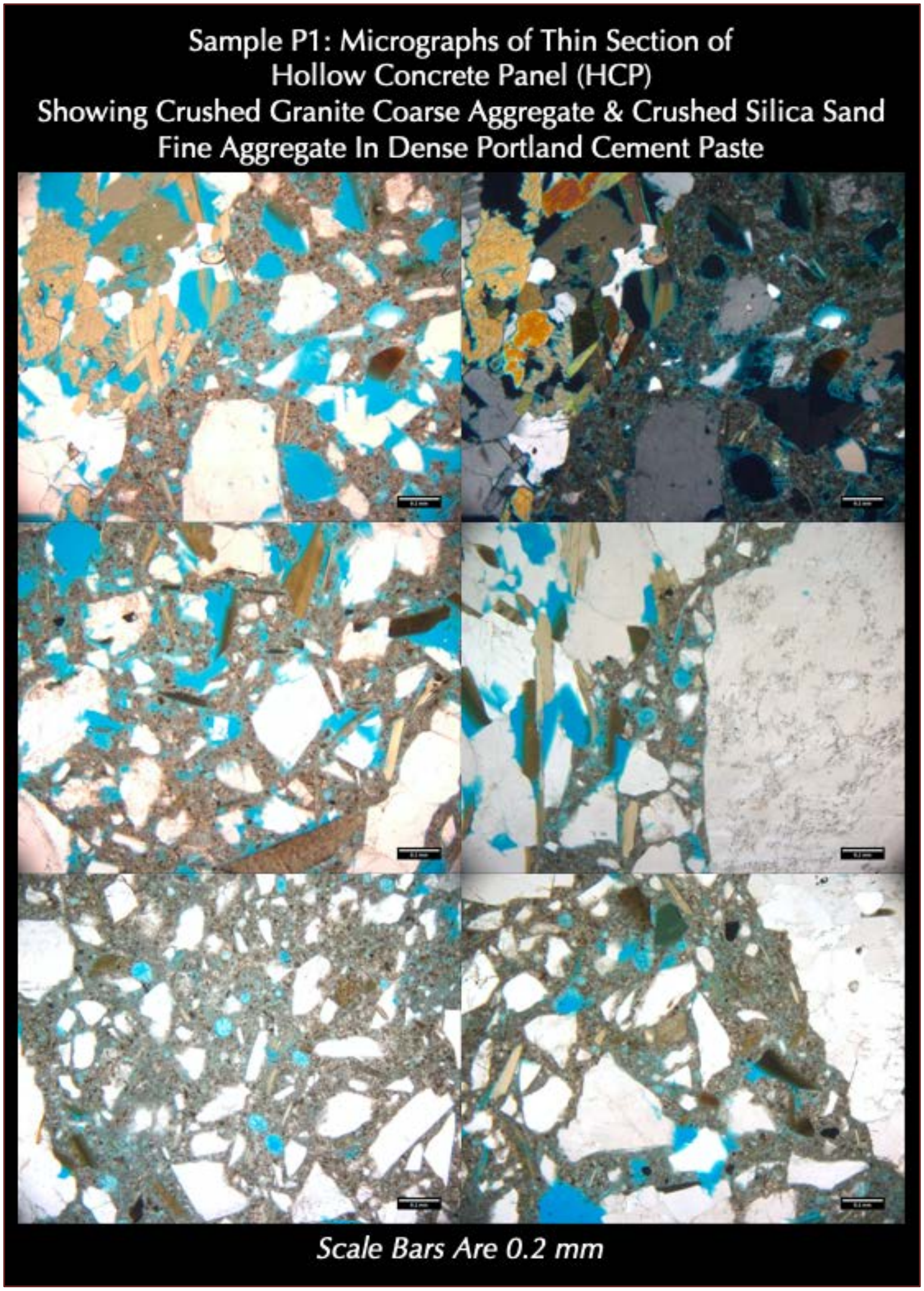

Figure 41: Micrographs of thin section of hollow core panel (HCP) in P-1 showing the crushed granite coarse aggregate particles having quartz, alkali feldspar (microcline, and orthoclase), and plagioclase (albite) mineralogies of granite with minor muscovite and biotite flakes, showing typical coarse-grained intergranular crystalline texture of granite, and crushed silica sand fine aggregate particles having major amounts of quartz and subordinate amounts of quartzite, granite, feldspar particles and dense interstitial Portland cement paste without any spherical particles of residual fly ash found in the RCS component. Notice many entrapped air voids highlighted by blue epoxy are lined or filled with fibrous secondary ettringite deposits in the bottom left photo indicating the presence of moisture in HCP during service.

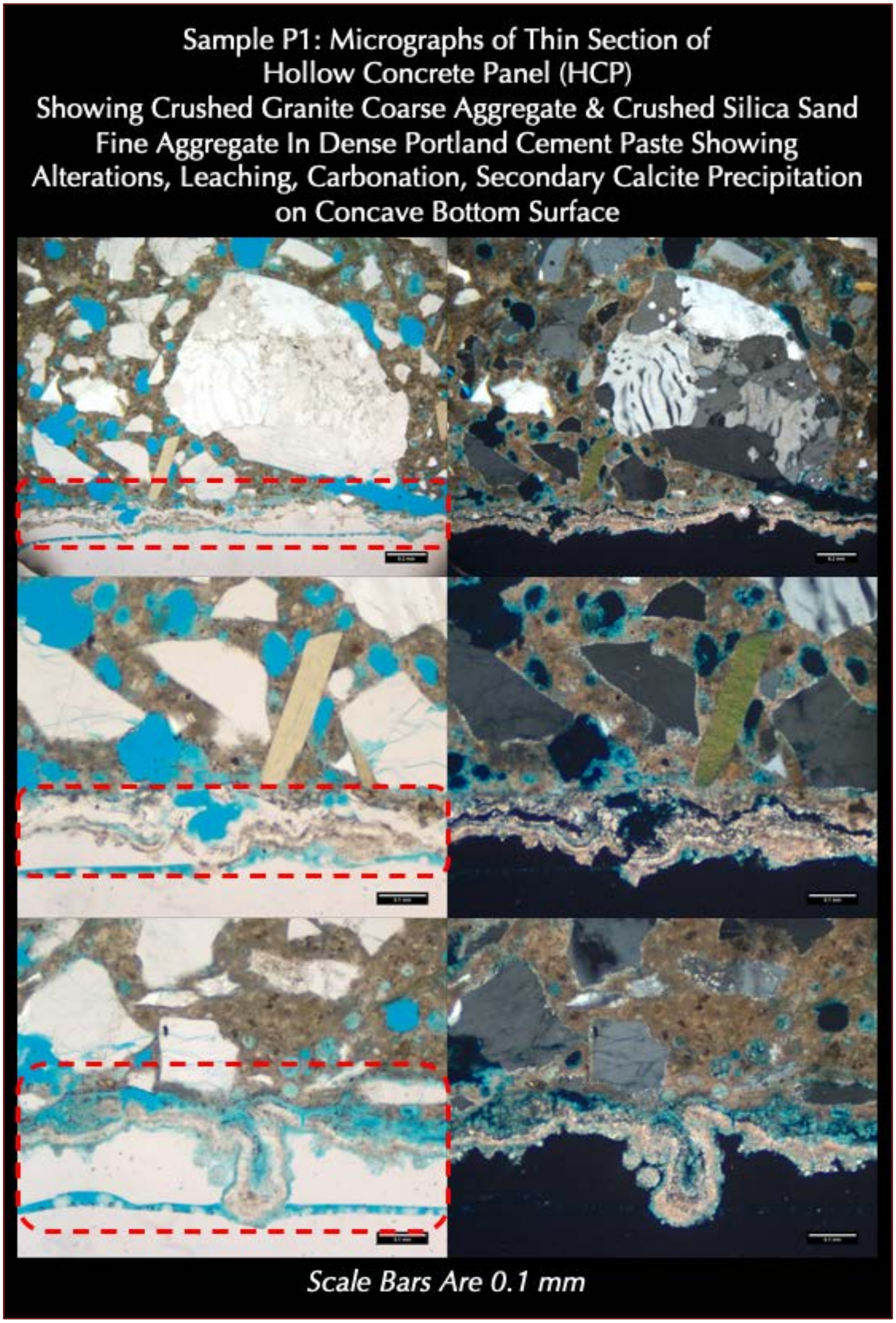

Figure 42: Micrographs of thin section of hollow core panel (HCP) in P-1 showing the altered zone at the weathered brown underside surface end consisting of coarsely crystalline secondary calcite precipitates at the very end (which is boxed at left column photos) above a leached paste zone, which, in turn, is followed by a carbonated paste in the interior of HCP. All these alterations are confined to within 3 to 5 mm of the weathered altered underside surface.

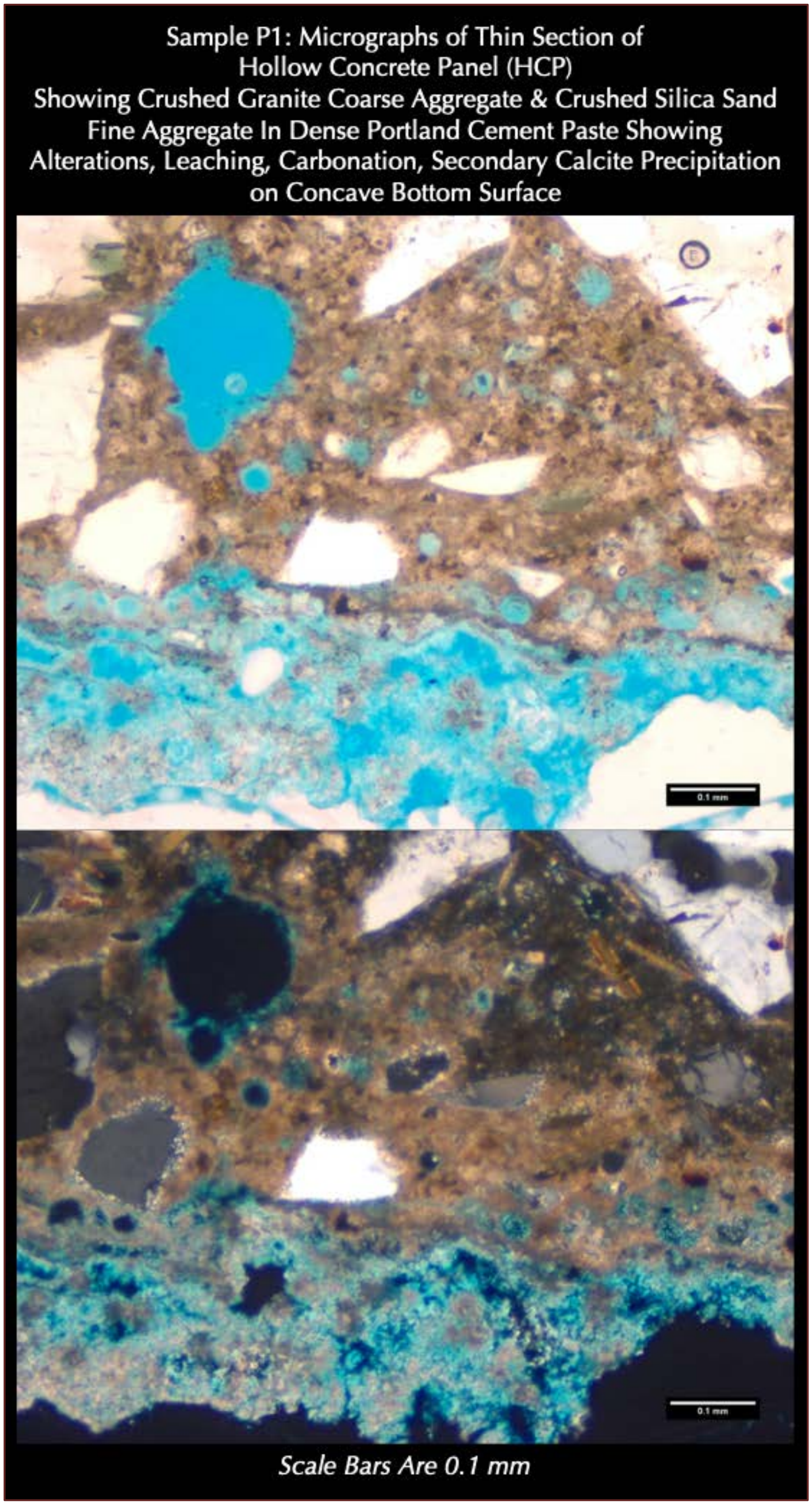

Figure 43: Micrographs of thin section of hollow core panel (HCP) in P-1 showing the altered zone at the weathered brown underside surface end consisting of coarsely crystalline secondary calcite precipitates at the very end above a leached paste zone, which, in turn, is followed by a carbonated paste in the interior of HCP. All these alterations are confined to within 3 to 5 mm of the weathered altered underside surface.

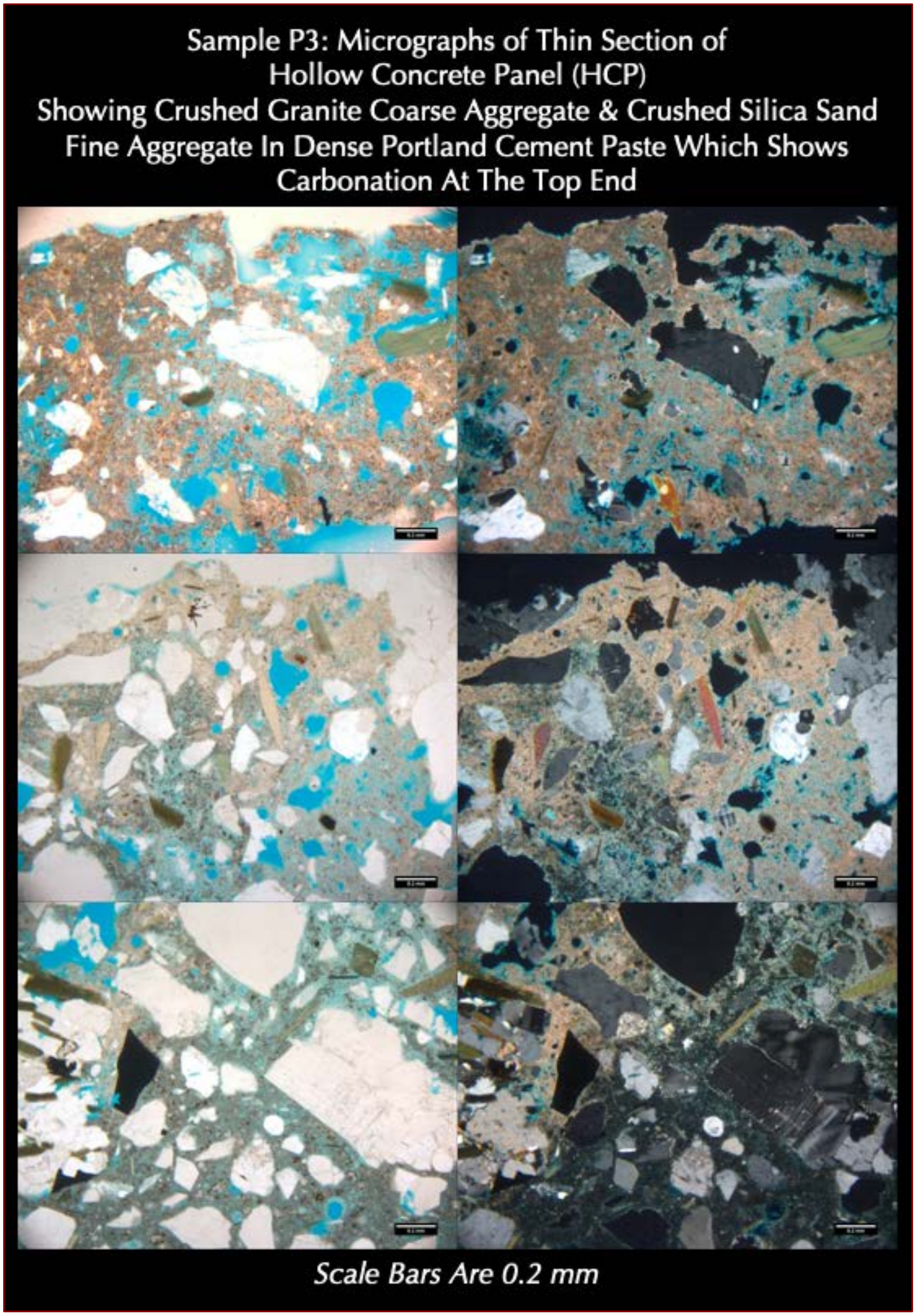

Figure 44: Micrographs of thin section of hollow core panel (HCP) in P-3 showing the crushed granite coarse aggregate particles having quartz, alkali feldspar (microcline, and orthoclase), and plagioclase (albite) mineralogies of granite with minor muscovite and biotite flakes, showing typical coarse-grained intergranular crystalline texture of granite, and crushed silica sand fine aggregate particles having major amounts of quartz and subordinate amounts of quartzite, granite, feldspar particles and dense interstitial Portland cement paste without any spherical particles of residual fly ash found in the RCS component. Notice golden yellow interference color of carbonated paste at the altered weathered brown surface of HCP that are highlighted in the right column XPL images.

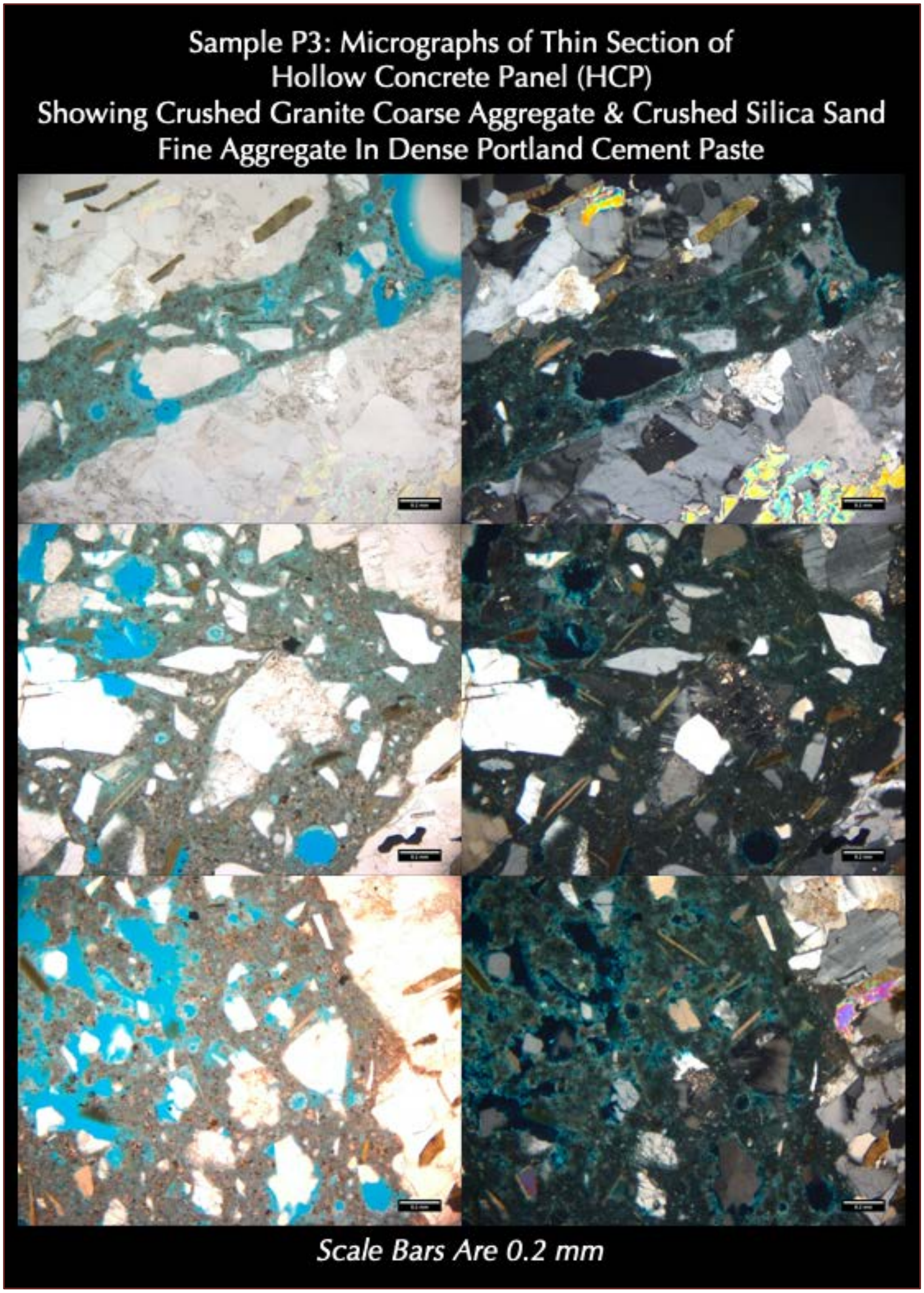

Figure 45: Micrographs of thin section of hollow core panel (HCP) in P-3 showing the crushed granite coarse aggregate particles having quartz, alkali feldspar (microcline, and orthoclase), and plagioclase (albite) mineralogies of granite with minor muscovite and biotite flakes, showing typical coarse-grained intergranular crystalline texture of granite, and crushed silica sand fine aggregate particles having major amounts of quartz and subordinate amounts of quartzite, granite, feldspar particles and dense interstitial Portland cement paste without any spherical particles of residual fly ash found in the RCS component.

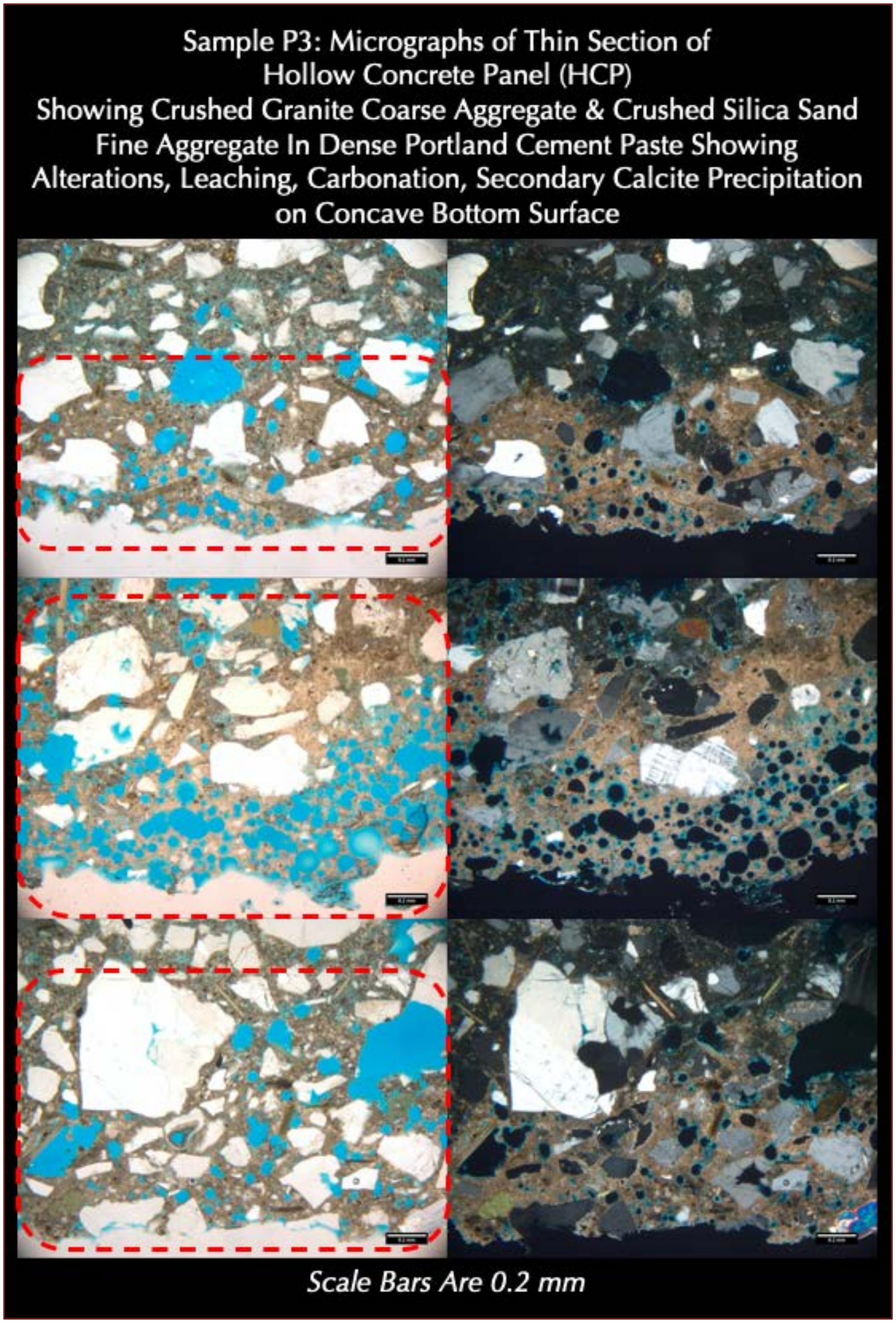

Figure 46: Micrographs of thin section of hollow core panel (HCP) in P-3 showing the altered zone at the weathered brown underside surface end consisting of coarsely crystalline secondary calcite precipitates at the very end (which is boxed at left column photos) above a leached paste zone, which, in turn, is followed by a carbonated paste in the interior of HCP. All these alterations are confined to within 3 to 5 mm of the weathered altered underside surface. Notice some frothy-textured excessively air-entrained paste at the very bottom of altered underside best seen in the middle row images due to interaction with the moist exhaust materials inside the HCP.

REINFORCED CONCRETE SLAB (RCP)

Coarse Aggregate

Coarse aggregate in the reinforced concrete roof top slab component in Cores C-1 and C-2 is crushed volcanic rocks of nominal 1 in. (25 mm) in size consisting of basalt-andesite-trachyte series of basic volcanic rocks showing typical ferromagnesian mineralogies of pyroxene and plagioclase phenocrysts in finer-grained glassy and microcrystalline ground mass of pyroxene, plagioclase, and glass to define the typical porphyritic textures. Coarse aggregate particles are variably altered to give a greenish tone of some of the particles, angular, dense, hard, equidimensional to elongated, unaltered, uncoated, and uncracked. There is no evidence of alkali-aggregate reactions or any other potentially deleterious reactions of crushed volcanic rock coarse aggregates found in the RCS component in Cores C-1 or C-2.

Fine Aggregate

Fine aggregates in the reinforced concrete roof top slab component in Cores C-1 and C-2 is crushed silica sand of nominal $^3/_8$ in. (9.5 mm) in size consisting of major amount of crushed quartz and subordinate amounts of crushed quartzite, granite, feldspar, and other siliceous rocks. Fine aggregate particles are angular, dense, hard, equidimensional to elongated, unaltered, uncoated, and uncracked. There is no evidence of alkali-aggregate reactions or any other potentially deleterious reactions of crushed sand fine aggregates found in the RCS component in Cores C-1 or C-2.

Properties and Compositions of Aggregates	Cores C-1 and C-2
Coarse Aggregate	
Types	Crushed volcanic rocks
Nominal maximum size (in.)	1 in. (25 mm)
Rock Types	Basalt-andesite-trachyte series of basic volcanic rocks showing typical ferromagnesian mineralogies of pyroxene and plagioclase phenocrysts in finer-grained glassy and microcrystalline ground mass of pyroxene, plagioclase, and glass to define the typical porphyritic textures
Angularity, Density, Hardness, Color, Texture, Sphericity	Variably altered to give a greenish tone of some of the particles, angular, dense, hard, equidimensional to elongated
Cracking, Alteration, Coating	Unaltered, Uncoated, and Uncracked
Grading & Distribution	Well-graded, well-distributed
Soundness	Sound
Alkali-Aggregate Reactivity	None
Fine Aggregates	
Types	Crushed silica sand
Nominal maximum size (in.)	$^3/_8$ in. (9.5 mm)

Properties and Compositions of Aggregates	Cores C-1 and C-2
Rock Types	Major amount of crushed quartz and subordinate amounts of crushed quartzite, granite, feldspar, and other siliceous rocks
Cracking, Alteration, Coating	Clear to gray, subangular to rounded, dense, hard, equant to elongated
Grading & Distribution	Well-graded and Well-distributed
Soundness	Sound
Alkali-Aggregate Reactivity	None

Table 2: Properties of coarse and fine aggregates of concrete in RCS component in Cores C-1 and C-2.

Paste

Properties and composition of hardened cement paste in the RCS are summarized in Table 3. Paste is beige gray in RCP component in Cores C-1 and C-2, moderately dense, and moderately hard. Freshly fractured surfaces have subvitreous lusters and subconchoidal textures. Residual and relict Portland cement particles are present and estimated to constitute 10 to 12 percent of the paste volumes in the interior bodies. Distributed throughout the paste are a few fine, spherical, clear, dark brown to black glassy particles of fly ash having the fineness of Portland cement. Hydration of Portland cement is normal.

Properties and Compositions of Paste	Cores C-1 and C-2
Color, Hardness, Porosity, Luster	Paste is beige gray in RCP component in Cores C-1 and C-2, moderately dense, and moderately hard. Freshly fractured surfaces have subvitreous lusters and subconchoidal textures
Residual Portland Cement Particles	Normal, 6 to 8 percent by paste volume
Calcium hydroxide from cement hydration	Normal, 10 to 14 percent by paste volume
Pozzolans, Slag, etc.	Fly ash having the fineness of Portland cement
Water-cementitious materials ratio (*w/cm*), estimated	0.45 to 0.50
Cementitious materials content (bags per cubic yard)	6 to 6$^{1}/_{2}$ bags per cubic yard, of which 10 to 15 percent is estimated to be fly ash
Secondary Deposits	None
Depth of Carbonation, mm	2 to 3 mm from exposed ends
Microcracking	None except short, discontinuous gaps or incipient delamination at the top $^{1}/_{8}$ in. of densified finished surface regions of RCS in both cores, especially visible in Core C-2
Aggregate-paste Bond	Tight except at areas of air-void clustering due to excessive air entrainment to weaken the bonds
Bleeding, Tempering	None
Chemical deterioration	None

Table 3: Proportions and composition of hardened cement paste in the RCS component in Cores C-1 and C-2.

Air

The reinforced concrete roof top slab (RCS) component is excessively air entrained where air occurs as: (i) numerous fine discrete, spherical and near-spherical voids having sizes of up to 1 mm, and (ii) a few coarse, near-spherical and irregularly shaped voids of sizes coarser than 1 mm. The former voids are characteristic of entrained air and the latter ones are characteristic of entrapped air. Figures 23 and 24 show micrographs of lapped cross sections of RCS where excessive air entrainment in concrete are seen. High air, and clustering of voids along aggregate-paste interfaces are seen due to excessive air, which can potentially reduce the overall compressive strength of concrete. Air content is estimated to be 8 to 10 percent.

Due to high air content the cast-in-place concrete in RCS was sticky, which has increased the difficulty to achieve a desirable fine broom-finish of the surface. Hence, there is evidence of prolonged finishing and finishing-induced densification of surface to create fine, short, elongated, discontinuous gaps or separations as incipient delamination within the top $^{1}/_{8}$ in. of the finished surface, which has the potential to develop large-scale delamination and separation of the densified finished surface from the interior main body. However, no such evidence of complete detachment of the air-free or low-air finished surface from the excessively air-entrained interior body is found in the RCS component in Cores C-1 or C-2.

Therefore, excessive air in RCS has not only affected the overall compressive strength of concrete both from high air and the weakened aggregate-paste bond due to clustering of air at the aggregate-paste interfaces, but also affected the finishing operations to develop the potential for incipient delamination of the finished surface from the main body.

HOLLOW CORE PANEL (HCP)

Coarse Aggregate

Coarse aggregate in the hollow core panel component in Samples C1, C-2, P-1, and P-3 are all compositionally similar consisting of crushed granite having a nominal maximum size of $^{1}/_{2}$ in. (12.5 mm). Particles are angular, dense, hard, medium brown, equidimensional to elongated, well-graded, and well-distributed. Granite shows typical mineralogies of quartz, alkali feldspar (microcline many showing typical crisscross twins, and orthoclase), plagioclase (albite), and mica (muscovite and biotite flakes) all arranged in coarse-grained equigranular crystalline texture. There is no evidence of alkali-aggregate reactions or any other potentially deleterious reactions of crushed granite coarse aggregates found in the HCP components in any sample.

Fine Aggregate

Fine aggregates are compositionally similar crushed silica sands as found in the RCS component, having nominal maximum sizes of $^{3}/_{8}$ in. (9.5 mm) in size, consisting of major amount of crushed quartz and subordinate amounts of crushed quartzite, granite, feldspar, and other siliceous rocks. Fine aggregate particles are angular, dense, hard, equidimensional to elongated, unaltered, uncoated, and uncracked. There is no evidence of alkali-aggregate reactions or any other potentially deleterious reactions of crushed sand fine aggregates in the HCP component.

Properties and Compositions of Aggregates	HCP components in C-1, C-2, P-1, P-3
Coarse Aggregates	
Types	Crushed granite
Nominal maximum size (in.)	$^{1}/_{2}$ in. (12.5 mm)
Rock Types	Major amount of crushed quartz and subordinate amounts of crushed quartzite, granite, feldspar, and other siliceous rocks
Angularity, Density, Hardness, Color, Texture, Sphericity	Angular, dense, hard, dark gray, massive crystalline granular, coarse-grained textured, equidimensional to elongated
Cracking, Alteration, Coating	Unaltered, Uncoated, and Uncracked
Grading & Distribution	Well-graded, well-distributed
Soundness	Sound
Alkali-Aggregate Reactivity	None
Fine Aggregates	
Types	Crushed silica sand
Nominal maximum size (in.)	$^{3}/_{8}$ in. (9.5 mm)
Rock Types	Major amount of crushed quartz and subordinate amounts of crushed quartzite, granite, feldspar, and other siliceous rocks
Cracking, Alteration, Coating	Clear to gray, subangular to rounded, dense, hard, equant to elongated
Grading & Distribution	Well-graded and Well-distributed
Soundness	Sound
Alkali-Aggregate Reactivity	None

Table 4: Properties of coarse and fine aggregates of concrete in the HCP components in Cores C-1, C-2 and samples P-1, and P-3.

Paste

Properties and composition of hardened cement pastes are summarized in Table 5. Pastes in HCP components are dense, hard, medium gray. Freshly fractured surfaces have subvitreous lusters and subconchoidal textures. Residual and relict Portland cement particles are present and estimated to constitute 10 to 12 percent of the paste volumes in the interior bodies. Hydration of Portland cement is normal.

Properties and Compositions of Paste	HCP components in C-1, C-2, P-1, P-3
Color, Hardness, Porosity, Luster	Paste in the HCP component is medium gray, uniform in color tone throughout the interior except the lighter discolored paste at the 5 to 10 mm of the underside altered weathered brown surface region due to leaching, carbonation, alteration, and secondary calcite precipitation due to interactions with the materials during service. Freshly fractured surfaces in the interior bodies have subvitreous lusters and subconchoidal textures

Properties and Compositions of Paste	HCP components in C-1, C-2, P-1, P-3
Residual Portland Cement Particles	Normal, 6 to 8 percent by paste volume
Calcium hydroxide from cement hydration	Normal, 10 to 14 percent by paste volume
Pozzolans, Slag, etc.	None
Water-cementitious materials ratio (*w/cm*), estimated	0.40 to 0.45 in both cores
Cement content (bags per cubic yard)	7 to $7^1/_2$ bags per cubic yard
Secondary Deposits	A few entrapped air voids are lined with secondary ettringite deposits indicating the prolonged presence of moisture in the HCP component during service
Depth of Carbonation, mm	5 to 10 mm from the altered weathered underside surfaces
Microcracking	None except a fine horizontal microcrack found near the weathered underside surface in P-3
Aggregate-paste Bond	Tight
Bleeding, Tempering	None
Chemical deterioration	None

Table 5: Proportions and composition of hardened cement paste in the HCP component.

Air

Concretes in the HCP components in all samples are non-air-entrained having air contents estimated to be 2 to 3 percent which are all near-spherical and irregular-shaped entrapped air. Figures 22, 25, and 26 show the lack of any spherical entrained air voids and overall dense, well-consolidated and non-air-entrained nature of concrete in the HCP.

WATER-SOLUBLE ANION CONTENTS

Water-soluble chloride, sulfate and other anion contents from the altered underside region, mid-depth, and concave ends of HCPs in Samples P-1 and P-3 were determined by ion chromatography *a la* ASTM C 4327.

HCP	Depth (mm)	Chloride Content from Ion Chromatography (% Chloride by mass of concrete)	Sulfate Content from Ion Chromatography (% Sulfate by mass of concrete)
P-1	Altered Underside Mid-Depth Concave Side	0.0032 0.0026 0.0023	0.0926 0.1157 0.0210
P-3	Altered Underside Mid-Depth Concave Side	0.0032 0.0028 0.0027	0.1506 0.1624 0.0154

Table 6: Results of water soluble chloride and sulfate contents in HCPs determined by ion chromatography.

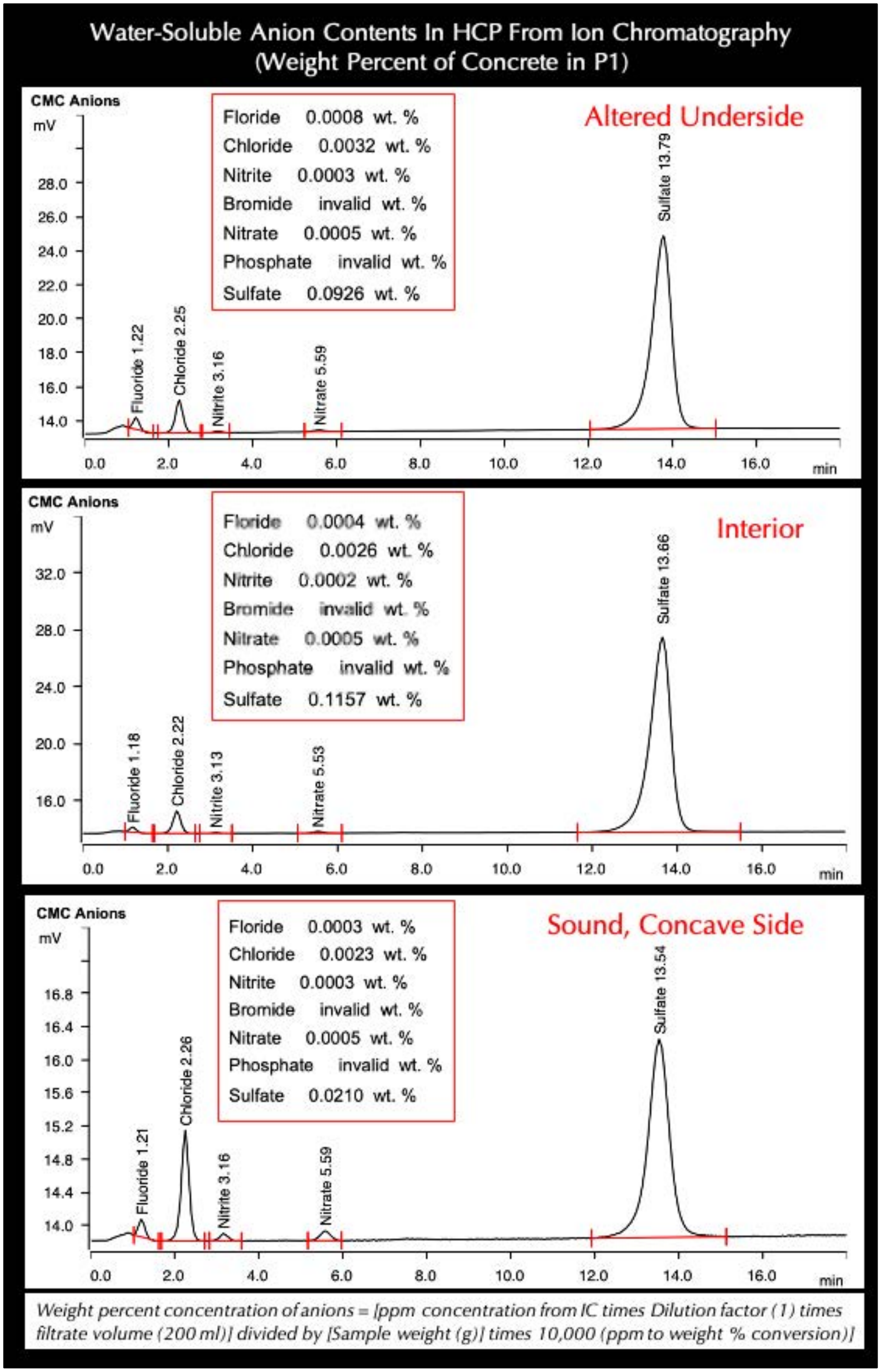

Figure 47: Ion chromatograms of water-soluble anions of filtrates of HCP in Sample P-1 from altered underside (top), mid-depth (middle), and concave end (bottom).

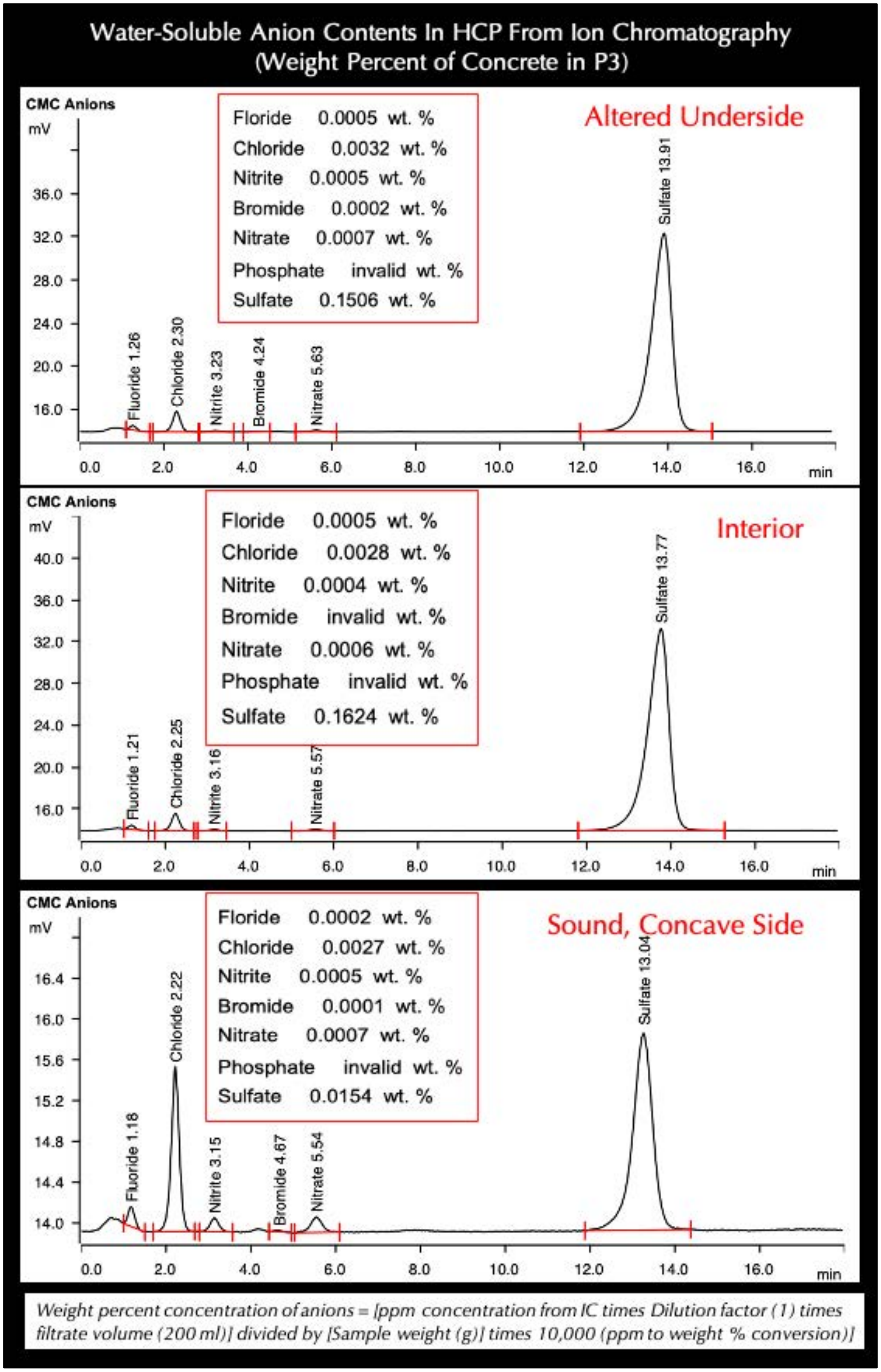

Figure 48: Ion chromatograms of water-soluble anions of filtrates of HCP in Sample P-3 from altered underside (top), mid-depth (middle), and concave end (bottom).

DISCUSSIONS

REINFORCED CONCRETE ROOF SLAB

The reinforced concrete roof top slab (RCS) component in Cores C-1 and C-2 are compositionally similar and made using: (a) crushed basalt-andesite-trachyte series of volcanic rock coarse aggregate of nominal 1 in. (25 mm) sizes that are angular, dense, hard, well-graded, well-distributed and present in sound conditions; (b) crushed silica sand fine aggregate; (c) binary cementitious blend of major amount of Portland cement and subordinate amount of fly ash having a cementitious materials content estimated to be equivalent to 6 to 6$^1/_2$ bags of Portland cement per cubic yard of which 10 to 15 percent is estimated to be fly ash, and water-cementitious materials ratios estimated to be 0.45 to 0.50 in the interior and slightly lower at the top $^1/_8$ in. of the densified finished surface region where finishing-induced densification has occurred to achieve the desired fine broom-finished surface of the roof top. The surface densification process was found to be an artifact of excessively air-entrained nature of RCS having an estimated 8 to 10 percent air, where high air has not only affected the overall compressive strength of concrete but also made the concrete sticky to cause prolonged finishing with the potential to leave short, discontinuous gaps or incipient delaminations between the densified no to low-air finished surface and excessively air-entrained interior body. Despite the reported lack of any surface delamination during field delamination survey petrographic examinations of RCS in Cores C-1 and C-2 showed the potential for incipient delamination as short gaps or separations beneath the densified finished surface.

HOLLOW CORE PANEL

The hollow core panel (HCP) component in Cores C-1 and C-2 and in Samples P-1 and P-3 are compositionally similar and made using: (a) crushed granite coarse aggregate of nominal $^1/_2$ in. (12.5 mm) sizes that are angular, dense, hard, well-graded, well-distributed and present in sound conditions; (b) crushed silica sand fine aggregate; and (c) a hardened Portland cement paste having cement contents similar in all samples and estimated to be 7 to 7$^1/_2$ bags per cubic yard, and water-cement ratios similar in all samples and estimated to be 0.40 to 0.45 in the interior bodies. Unlike RCS component, which is excessively air-entrained to have estimated 8 to 10 percent air, however, the HCP component in all samples show lack of air-entrainment having air contents estimated to be 2 to 3 percent.

CHEMICAL ALTERATIONS AT THE UNDERSIDE OF HOLLOW CORE PANEL

The undersides of HCP in P-1, P-2, and P-3 showed weathered brown altered, carbonated and leached paste exposing the aggregate particles relative to paste due to interactions with slurry materials which has affected the 5 to 10 mm zone of the underside. Coarsely crystalline secondary calcite precipitates are found at the underside surfaces of HCP which are precipitated on leached and carbonated and porous pastes extended to depths of 2 to 3 mm beyond which paste is denser but still shows carbonation before sound non-carbonated interior paste. Beyond the altered zone, the majority of the interior portions of HCP are present in dense, well-consolidated and sound conditions without any physical or chemical deterioration.

Chemical alterations of HCPs are found to be confined to the 10 mm of underside beyond which the interior concretes showed no alterations of paste such as softening, increasing porosity from leaching or carbonation, which are all found only at the underside altered zones. Water-soluble chloride contents are consistent through the thickness of HCPs in Samples P-1 and P-3, but water-soluble sulfate contents showed a factor of 5 to 10 increase towards the mid-depth and altered zones compared to the sound concave interiors due to the reported exposures to hydrogen sulfide gas and related sulfate exposures during service.

CRACKING

Major vertical crack extended through the entire thickness of RCS and HCP is seen in Core C-2 where the RCS component is well-bonded to HCP. By contrast, no cracking is found in RCS or HCP components in Core C-1 where the two components are completely de-bonded. Petrographic examinations of RCS and HCP found no evidence for any physical or chemical deterioration of concretes in these components to cause cracking. The vertical through-depth crack in Core C-2 is judged to be due to reasons not related to any deterioration in RCS and/or in HCP component. Perhaps, reasons such as the lack of control joints or expansion joints in the RCS has caused unaccommodative drying shrinkage cracking in RCS, which has extended not only through the RCS but also through the HCP component, especially where the two components are well-bonded as in the case of Core C-2.

REFERENCES

ASTM C 856 "Standard Practice for Petrographic Examination of Hardened Concrete," Vol. 4.02, ASTM International, West Conshohocken, PA, 2017.

ASTM C 1218 "Standard Test Method for Water-Soluble Chloride in Mortar and Concrete," Vol. 4.02, ASTM International, West Conshohocken, PA, 2017.

ASTM D 4327, "Standard Test Method for Anions in Water by Suppressed Ion Chromatography," Vol. 11.01, ASTM International, West Conshohocken, PA, 2019.

Jana, D., "Sample Preparation Techniques in Petrographic Examinations of Construction Materials: A State-of-the-Art Review," *Proceedings of the 28th Conference on Cement Microscopy (ICMA)*, 2006, pp. 23-70.

✪ ✪ ✪ END OF TEXT ✪ ✪ ✪

END OF REPORT[1]

[1] The CMC logo is made using a lapped polished section of a 1930's concrete from an underground tunnel in the U.S. Capitol.